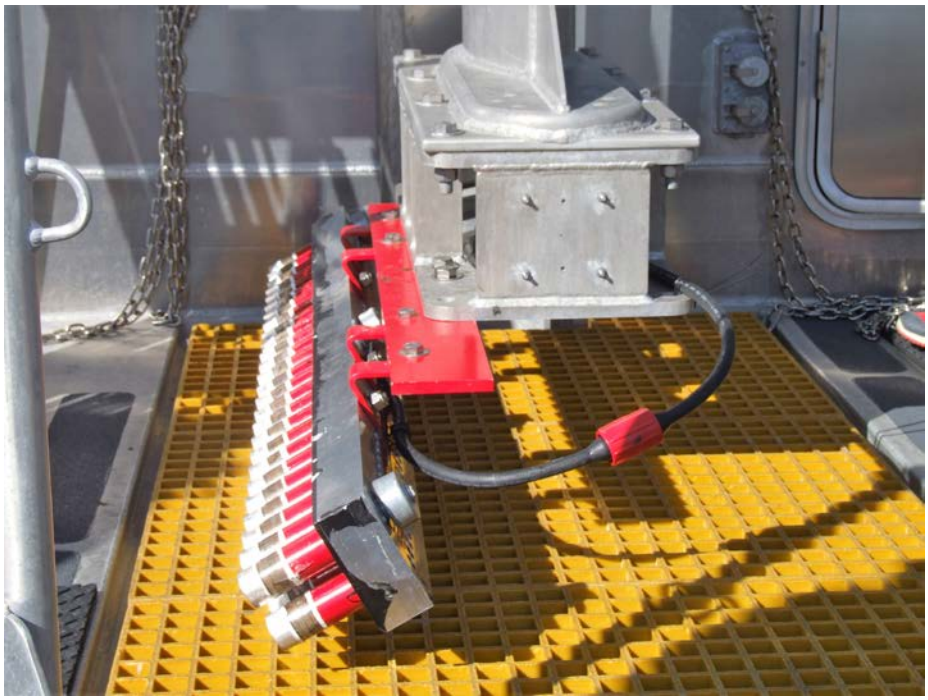

THE POSEIDON PROJECT:

Team Lead:
Langdon Tarbell

Team Members:
Alec Clemons, Graham Pirie, Mary Beth Sareault,
Naomie Clark, Paul Gesel, and Peter Abdu

Project Advisor:
Thomas Weber, PhD

Sea Grant
New Hampshire

Abstract

Ocean mapping and exploration is critical to understanding the world, its resources, and how they change over time. However, only a small percentage of the seafloor is mapped at high resolution. The objective of the Poseidon Project is to design and manufacture a low-cost portable device capable of mapping ocean bathymetry in real time at depths up to 2000 meters. Unique performance parameters require the device to operate in deep water regions with high resolution with a relatively small array. Performance specifications were met with a split aperture, four quadrant, side scan SONAR design. Application of the SONAR equation in the likely operating environment yielded crucial system design parameters. A 16-kHz system frequency was selected to achieve the depth requirement while maximizing bathymetric resolution. At the operating frequency, 13 transducers in each quadrant satisfied the minimum output signal intensity. Beam pattern analysis and portability considerations determined the transducer array geometry. The transducers were manufactured and assembled. Experimental data collected in the Chase Ocean Engineering tank determined the transmit voltage response, receive sensitivity, and beam pattern, allowing for calibration. The device was tested on the R/V Gulf Surveyor to create a map of the Piscataqua riverbed.

Acknowledgements

This project was sponsored by the University of New Hampshire Departments of Mechanical Engineering and Ocean Engineering. Funding was also provided through the Nation Science Foundation and the Center for Coastal and Ocean Mapping.

The Poseidon Project would not have been possible without the help and guidance of the following:

Thomas Weber, UNH Mechanical Engineering
Alexandra Padilla, UNH Ocean Engineering
Paul Lavoie, CCOM
Wendy Monroe, CCOM
Scott Campbell, UNH Machine Shop
Carlo Lanzoni, CCOM
Matt Rowell, CCOM
Daniel Tauriello, CCOM
Ronny Eichler, Northeast Precision Machining

This work is the result of research sponsored in part by the New Hampshire Sea Grant College Program through NOAA grant # NA10OAR4170082, and the UNH Marine Program.

Contents

Table of Figures

Table of Tables

I. Introduction

"With 95 percent of the ocean unmapped, more is known about the moon's surface than the ocean depths. Twelve men have walked on the moon, when only 2 men have been to the deepest part of the ocean, the Mariana Trench." (Israel, 2010)

Ocean mapping and exploration increases the understanding of the world and its resources, as well as how they change over time. However, only a small percentage, about 5%, of the seafloor is mapped at resolution comparable to that of the moon maps (Copley, 2014). SONAR [1] systems can be used for ocean exploration and mapping. There are numerous SONAR systems currently on the market. They range in price from as little as $1,000 for fish finder systems to more than $50,000 for high-tech side scan systems. The systems capable of mapping at greater depths are expensive, upwards of $50,000. These systems are cumbersome, some weighing more than 500 lbs.

The Poseidon Project's goals seek to solve the main problems facing ocean mapping; portability, cost, and resolution. A portable and cost effective system that can map at high resolution is highly marketable. The system created in this project, could increase the percentage of ocean floor mapped at high resolution. This system could even be a valuable resource in ocean mining. The earth's seafloor is full of minerals, such as copper, zinc and iron, that have not been tapped into. The Poseidon Project's system could be used to uncover the riches of the ocean floor as it can characterize the material of the ocean floor (Fin, 2010).

[1] SONAR stands for SOund Navigation And Ranging

II. Background

SONAR design uses sound waves to determine the depth of the ocean floor as well as detect and map objects on the floor itself. The sound waves bounce of the ocean floor and a fraction of the waves, the backscatter echoes, return to the SONAR system. The time elapsed between the sending out and receiving of the waves determines the distance of the ocean floor from the system (Side Scan Sonar, n.d.).

There are two types of SONAR systems, passive and active. Active SONAR sends out acoustic signals into the water. Some active systems are capable of then listening for a response echo to the emitted pulse. On the other hand, passive systems are only able to "listen". They do not send out signals, they only listen for sounds waves coming at the system. This is often used in military applications where stealth is important. For ocean floor mapping, an active SONAR that is equipped to listen to return signals is appropriate (What is Sonar?, 2014).

Active SONAR systems can be further categorized as side scan and multibeam systems. A side scan system is often used to find objects in the water and is attached at an angle to the vessel or can be dragged behind the vessel. Multibeam systems emit the acoustic signals directly below the vessel. Both are able of mapping the depths of the ocean floor below the vessel (What is Sonar?, 2014).

The objective of the Poseidon Project is to design and manufacture a low-cost portable device capable of mapping ocean bathymetry in real time at depths up to 2000 meters. An active split aperture, four quadrant, side scan SONAR design can accomplish this objective.

III. SONAR Theory

i. The SONAR Equation

To define parameters of a SONAR system, the SONAR equation, Equation 1, must be implemented. The SONAR equation quantifies the interaction of the generated acoustic waves, the medium through which they travel, and the target that they reflect off.

The SONAR equation is used to calculate ranges at which a target can be detected, while maintaining the signal-to-noise ratio, SNR, or the relative decibel difference between the incoming backscatter echoes and noise level above 10 dB. EL and NL are the received echo and noise levels, respectively. Both terms in the equation are given in units of decibels, or dB. A decibel is a logarithmic function of a ratio of acoustic pressure (units of N/m^2) or intensity (units of W/m^2). The denominator value is a reference value, which for this project is always with reference to 1 micro Pascal of pressure, while the numerator is the measured value of interest.

$$SNR = EL - NL \qquad \text{Equation 1.}$$

a. Echo Level

The echo level, defined as the total received backscatter signal intensity, is obtained with Equation 2. In this equation, SL is the source level, TL is the transmission loss, and TS is the target strength.

$$EL = SL - 2TL + TS \qquad \text{Equation 2.}$$

b. Source Level

SL is the source level, or the total decibel output of the acoustic signal created by the transducer array in the direction of the detected target, and is determined by transducer properties, number of transducers in the array, and electronic system parameters. Equation 3 is used to calculate the source level of the system. In this equation, 170.8 is an experimentally determined constant, P_{el} is the electrical power output of the system, and β is the average piezo efficiency or voltage to acoustic pressure efficiency of each transducer. P_{el} was chosen to be 1000 watts, from which the electrical system was designed. β was estimated to be about 25% for simulation purposes.

$$SL = 170.8 + 10log_{10}P_{el} + 10log_{10}\beta \qquad \text{Equation 3.}$$

c. Transmission Loss

TL is defined as transmission loss, a measure of energy loss experienced by an acoustic signal due to spreading and absorption during transmission. Because the

signal created by piston transducers is not emitted in a strict line or plane, but rather radiated in a complex pattern of directions, the signal pressure dissipates naturally as the signal travels further distances. The logarithmic nature of sound causes spreading losses to be a logarithmic function of travel range. As such, spreading losses are measured with Equation 4. The value r represents the range the signal is transmitted.

$$TL_s = 20log_{10}r \qquad \text{Equation 4.}$$

Absorption losses are due to resistance to the signal exerted by the medium through which it is travelling, shown in Equation 5. In this equation, α is the absorption coefficient of the transmission medium. The absorption coefficient is a value based on signal frequency, depth, as well as ambient temperature, salinity, and acidity. For ocean water, this value was approximated to be 2.018 dB/km (Francois & Garrison, 1982).

$$TL_a = \alpha r \qquad \text{Equation 5.}$$

From here the total transmission loss of the acoustic signal is defined as in Equation 6. In the echo level equation, Equation 2, the transmission loss term is multiplied by two. This is done because there are transmission losses as the signal travels both to and from the detected target.

$$TL = TL_s + TL_a \qquad \text{Equation 6.}$$

d. Target Strength

Now that that transmission losses have been defined, there is only one large portion of loss that has not been touched upon; losses within the target. When the signal reaches the target, some of the signal energy will get absorbed into the target and some will be reflected. Target strength is a measure of this reflection as a property of the target itself, given in units of negative decibels. A value of this can be calculated generally using Equation 7 where I_i is the intensity incident to the target and I_r is the intensity reflected from the target. The ratio of the two is dependent on material and signal properties.

$$TS = 10log_{10}\frac{I_r}{I_i} \qquad \text{Equation 7.}$$

Equation 8 shows, more specifically, the target strength dependencies on the material and signal separately. In this equation, S_b is defined as the seafloor backscatter strength. This is an inherent property of the seabed, defined experimentally as a function of incident material and angle (Jackson & Richardson, 2011). The value of A is the total area of the beam interacting with the seafloor at any given point in time, as defined in Equation 9. In this equation, c is the speed of sound in water, defined as approximately 1528 m/s, and τ is the pulse length in seconds.

$$TS = S_b + 10\log_{10} A \qquad \text{Equation 8.}$$

$$A = (\theta_{3dB} r)(\frac{c\tau}{2sin\theta_i}) \qquad \text{Equation 9.}$$

To further describe target strength, Figures 1 and 2 are shown below as visual aids. The $c\tau/2$ represents the outgoing signal pulse length in meters, divided by two to note that the received signal will travel both to and from the target, where the total pulse length will be equal to $c\tau$. This value is then divided by $\sin(\theta i)$ to project the beam onto the seafloor. The width of the beam is equivalent to θ_{3dB}, multiplied by the transmitted range, r, at which the signal at any given time first meets the seafloor.

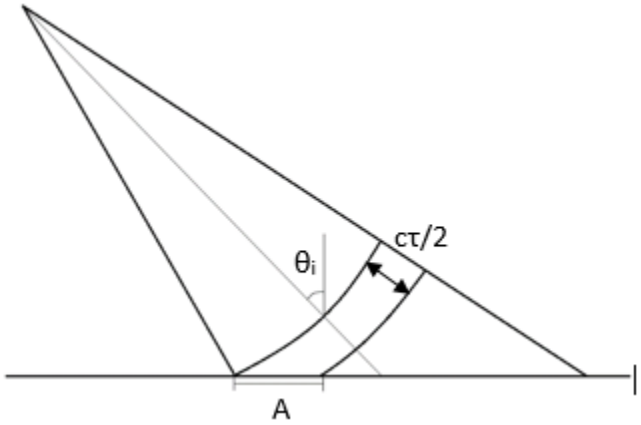

Figure 1: Side view of signal beam

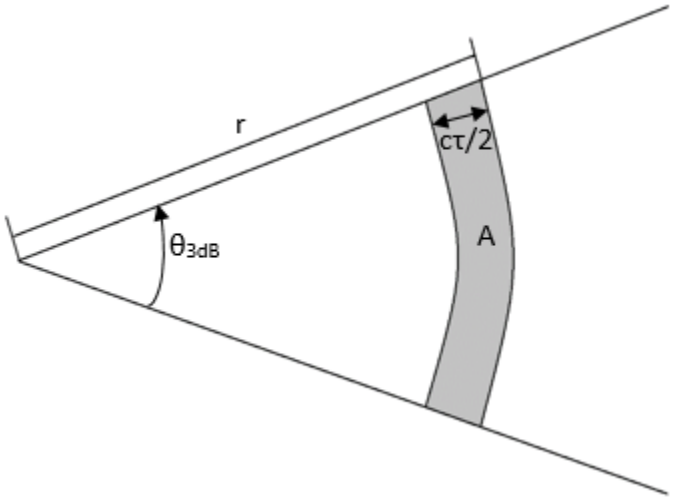

Figure 2: Top-down view of signal beam

From here, the target strength is fully defined, shown in Equation 10. The meaning of θ_{3dB}, though simple in concept, takes a much deeper understanding of acoustics to define. This derivation and more will be covered in the following sections.

$$\boldsymbol{TS = S_b + 10\log_{10}(\frac{\theta_{3dB} r c \tau}{2 sin\theta_i})} \qquad \text{Equation 10.}$$

e. Directivity Index

Up to this point, the SONAR model only describes the sound created and received in the same direction as the transducer piston motion. Taking out this assumption, the SONAR equation takes on a new form shown in Equation 11.

$$\text{SNR} = \text{EL} - (\text{NL} - \text{DI}) \qquad \text{Equation 11.}$$

DI is the directivity index, a receive property that denotes directionality of an array. Directivity index is used to eliminate incoming noise from certain directions, and defines how an array interacts with targets at different angles. This directionality is best described by comparing a spherical transducer, like that in hydrophones used during testing, to the cylindrical piston cylinder. Because of the spherical transducer's symmetrical nature, it receives acoustic waves omnidirectionally. If the piston transducer is placed in the same omnidirectional pressure field as the spherical transducer, the shape of the piston transducer allows only pressures acting along the plane at the top of the cylinder to be received. Equation 12 generally defines the directivity index where I_{avg} is the average signal intensity received by the array, and I_{max} is the intensity received if the detected target were directly in front of the array. The reason it is denoted with 'max' in the subscript is because, if properly built, a line array such as the one that was created will output the most acoustic pressure along a plane perpendicular to the width of the array. To understand this characteristic, it is necessary to explore the concepts behind the directional dependencies.

$$\boldsymbol{DI = 10log_{10}\frac{I_{max}}{I_{avg}}} \qquad \text{Equation 12.}$$

f. Directional Dependency

To delve further into how direction changes sending and receiving signal properties, first consider a continuous line array from length x = -L/2 to length x = L/2, emitting signals over distances r and r' to a single point of pressure. This is shown in Figure 3.

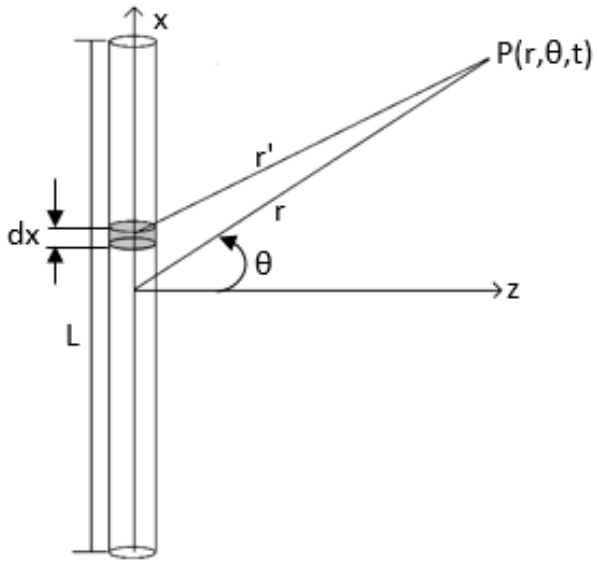

Figure 3: Depiction of ideal continuous line array

The line array is then split into simple sources. These sources are infinitely small and emit an ideal spherical acoustic pressure field. The characteristics of these sources allow an approximation of total pressure distribution along the line array to be made using Equation 13. In this equation, A is the signal amplitude, ω is equal to 2πf, with f representing the signal frequency, and k is the wave number, equal to 2π/λ, where λ is the signal wavelength.

$$P(r,\theta,t) = \int_{-\frac{L}{2}}^{\frac{L}{2}} \frac{A}{r'} e^{j(\omega t - kr')} \qquad \text{Equation 13.}$$

Assuming r >> L, it is possible to define r' as a function of r, Equation 14.

$$r' = r - sin\theta \qquad \text{Equation 14.}$$

Substituting Equation 14 into Equation 13 and simplifying the integral by taking out the constants gives Equation 15.

$$P(r,\theta,t) = \frac{A}{r} e^{j(\omega t - kr)} \int_{-\frac{L}{2}}^{\frac{L}{2}} e^{jkxsin\theta} \qquad \text{Equation 15.}$$

Evaluating this integral over the length of the line array gives Equation 16.

$$P(r,\theta,t) = \frac{AL}{r} e^{j(\omega t - kr)} \frac{\sin(\frac{kL}{2} sin\theta)}{(\frac{kL}{2} sin\theta)}$$ Equation 16.

From Equation 16, the directional factor is then defined as shown in Equation 17. In this equation, sinc is the sine cardinal function or the sampling function. This is a commonly used function in signal processing. The sinc function is characterized by the limitations shown in Equation 18.

$$H(\theta) = sinc(\frac{kL}{2} sin\theta)$$ Equation 17.

$$sincx = \begin{cases} 1 & for\ x = 0 \\ \frac{sinx}{x} & for\ x \neq 0 \end{cases}$$ Equation 18.

Figure 4 shows how the directional factor generally behaves.

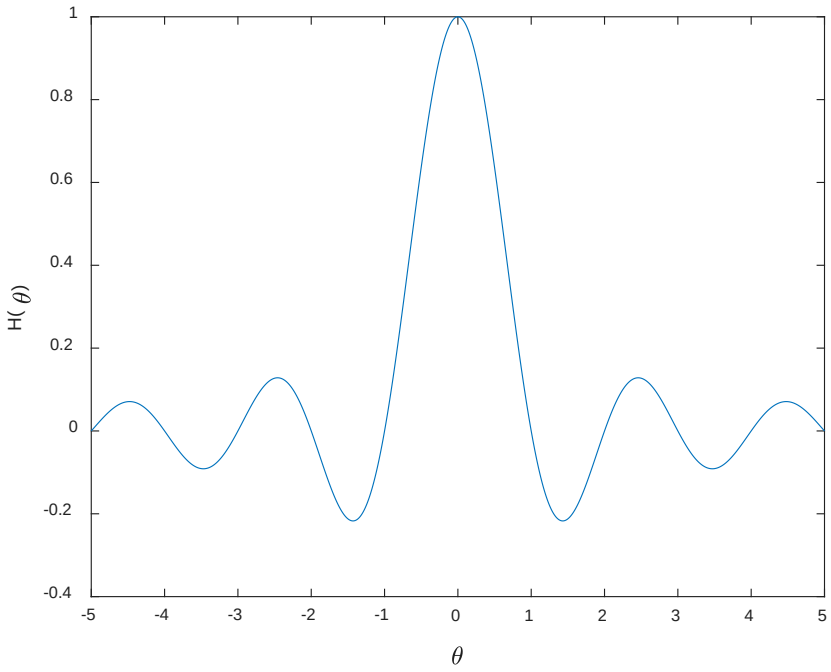

Figure 4: Plot of directional factor

As seen in Figure 4, the max value of the directional factor is 1, and it oscillates in a decreasing fashion about 0 as θ increases or decreases. This behavior is related to radiated power. Consider a source emitting a signal that hits a target, ds, with an intensity, I, at distance R as shown in Figure 5.

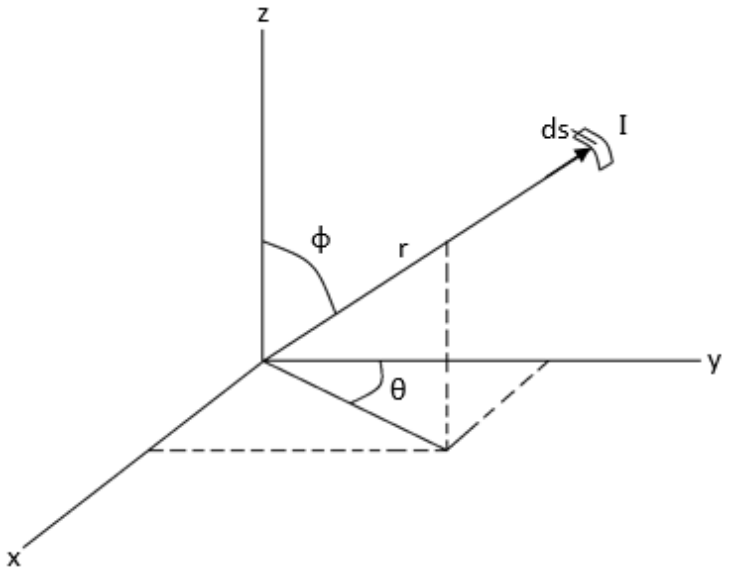

Figure 5: Radiated power from an acoustic source

From Figure 5, the radiated power emitted from this source shown in as a function of angles θ and φ is obtained. This is shown in Equation 19.

$$\pi_p = \int Ids = \iint_0^{2\pi} \frac{|P|^2}{2\rho_o c}(r^2 sin\theta \, d\theta d\phi) \qquad \text{Equation 19.}$$

The magnitude of the pressure is defined using Equation 20.

$$|P| = P_{max} H(\theta, \phi) \qquad \text{Equation 20.}$$

Substituting Equation 19 into Equation 20, the radiated power is written as shown in Equation 21.

$$\pi_p = \frac{r^2 P_{max}^2}{2\rho_o c} \int_0^{2\pi} \int_0^{\pi} H^2(\theta, \phi) sin\theta d\theta d\phi \qquad \text{Equation 21.}$$

The radiated power is related to the average emitted intensity by equating it to the radiated power from an omnidirectional source, Equation 22.

$$I_{avg} = \frac{\pi_p}{4\pi r^2} = \frac{P_{max}^2}{8\rho_o c} \int_0^{2\pi} \int_0^{\pi} H^2(\theta, \phi) sin\theta \, d\theta d\phi \qquad \text{Equation 22.}$$

Recall Equation 23, the equation for directivity index.

$$\text{DI} = 10 \log_{10} \frac{I_{max}}{I_{avg}} \qquad \text{Equation 23.}$$

Substituting in the definition of average emitted intensity, the directivity index is fully defined in Equation 23 as a function of both θ and φ.

$$DI = 10\log_{10}\left(\frac{4\pi}{\int_0^{2\pi}\int_0^{\pi} H^2(\theta,\phi)sin\theta\, d\theta d\phi}\right) \quad \text{Equation 23}$$

Solving Equation 23 with the geometry of a continuous line array gives Equation 24, the directivity index used for this project, assuming L >> λ. Though not the same for a discretely spaced array like the one used in this project, this is just an approximation used for modeling purposes.

$$DI = 20\log_{10}\frac{2L}{\lambda} \quad \text{Equation 24}$$

ii. Beam Pattern

The beam pattern is defined as the overall pressure distribution around a source emitting an acoustic signal. The beam pattern not only describes the amplitudes of pressure being emitted from a transducer array, but also gives information about the sensitivity of the array to pressures incoming from all directions. Not coincidentally, the directional sensitivity is the same for both the transmission and receive sides of operation. The beam pattern is directly related to the directional factor in Equation 25.

$$b(\theta) = 20\log_{10} H(\theta) \quad \text{Equation 25}$$

Plotting the beam pattern as a function of θ results in Figure 6. There are a few things to note in the plot. The plot shows the directional factor, as shown in Figure 4, in a dB scale. This is clearly shown as the peak in Figure 6 has been shifted to 0 when compared with that in Figure 4. Furthermore, each inflection point of the directional factor plot is now shown as an asymptote approaching negative infinity. The vertical axis at zero degrees is called the maximum response axis, as this is the direction in which the pressure distribution emitted by an acoustic source reaches its largest magnitude. As θ changes, so will the pressure distribution, visualizing the directional dependence of acoustic signals.

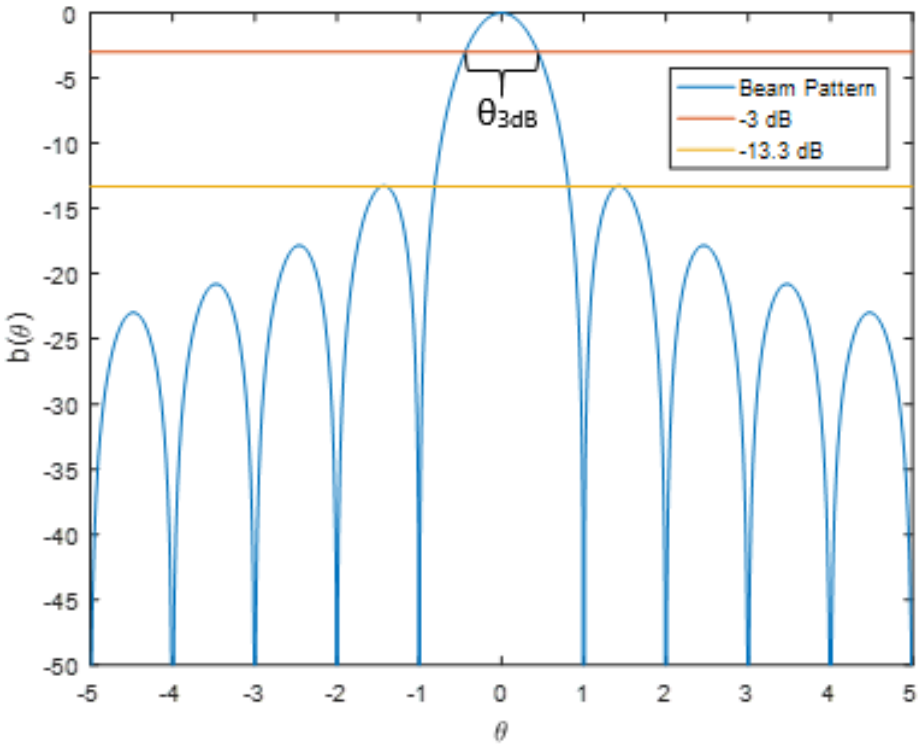

Figure 6: General plot of beam pattern

Each arc in Figure 6 is called a lobe. The primary lobe is the lobe about zero degrees, with the side lobes surrounding it on either side. A point of interest is side lobe level, or SLL, defined as the degree values at which the signal is 13.3 dB below the maximum decibel level. By going down -3dB on the plot, the degree difference between each point of the beam at this decibel level is defined as the beam width, or θ_{3dB}. This value is physically visualized in Figure 2 in the target strength section of the report, and is estimated to be $50\lambda/L$ for estimation purposes.

iii. SONAR model

With signal transmission properties, receive characteristics, and directional dependencies have been accounted for, the SONAR model used for this project is complete. Listed below in Table 1 and Table 2 are properties that were either assumed, or were calculated, to create the SONAR model. The model was based upon operating at the maximum goal depth of 2000m.

Table 1. List of signal properties

Operating Frequency	15 kHz
Wavelength	0.1019 m
Pulse length (time)	0.0167 s
Pulse length (distance)	3.8462°
Signal waves per pulse	250
Beam Width	25.4667 m

Signal Bandwidth	60 Hz
Resolution	3419 m^2

Table 2. Estimated send and receive characteristics of array

Source level	208.93 dB
Transmission loss	120.57 dB
Echo level	38.63 dB
Noise level	42.78 dB
Directivity index	14.15 dB
Signal-to-noise ratio	~10

Figure 8 below is the result of the model with the parameters from Table 1 and Table 2, plotted using MATLAB. The red line marks 2000m depth. Each contour line in Figure 8 represents the estimated horizontal and vertical detection ranges of various materials, ranging from clay to rough rock, for signal transmission angles ranging from 0˚ to 89˚. Each material has their own backscatter strength, with clay having the smallest, and rough rock having the largest target strengths. The maximum horizontal detection ranges of rough rock and clay at 2000m depth were defined as the inner and outer swath limits, respectively. These values are shown in Figure 8 as the furthest left and right intersection points with the 2000m depth line. The model was also run at 20kHz to understand the effects of operating frequency on detection ranges. Estimations of inner and outer swath limits for both frequencies were generated by the SONAR model, and are listed in Table 3.

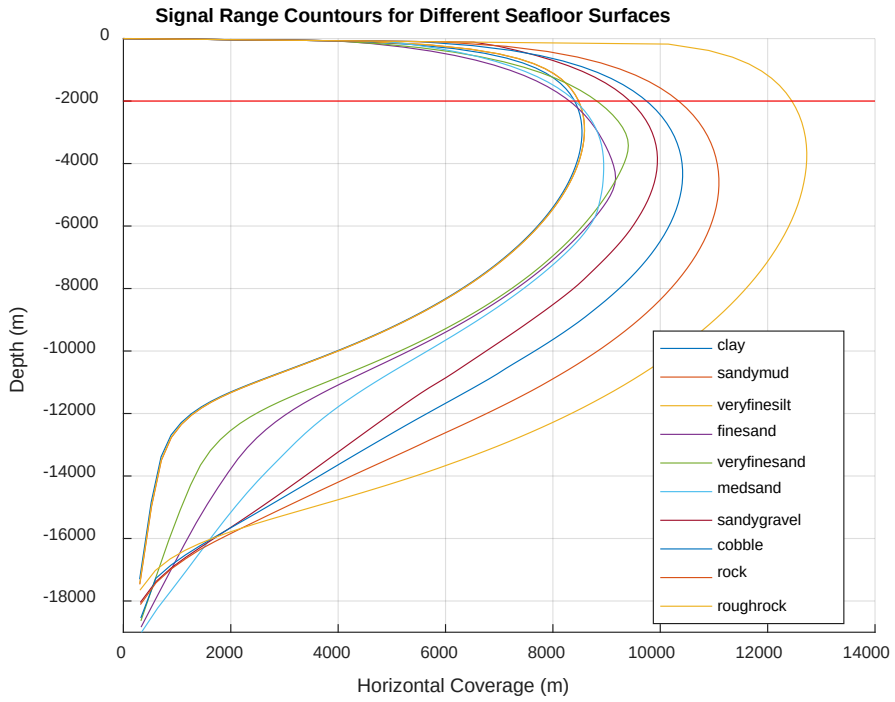

Figure 7. Model of SONAR performance

Table 3. Inner and outer swath limits of 15 kHz and 20 kHz signals

Operating Frequency [Hz]	Inner Swath Limit [m]	Outer Swath Limit [m]
15k	8373	12440
20k	7991	12100

Based on the findings in Table 3, the lower the operating frequency, the larger the detection range of the seafloor. Based on this, the operating frequency was chosen to be 15kHz. The design and manufacturing of the project was then based around this operating frequency. After full assembly, the transducers operated at an average 16kHz. The final estimations of inner and outer swath limits at the actual signal frequency are shown in Table 4.

Table 4. Inner and outer swath limits at 16 kHz

Operating Frequency [Hz]	Inner Swath Limit [m]	Outer Swath Limit [m]
16k	8285	12370

iv. Phase Differencing

The final concept needed by the SONAR system to create seafloor bathymetry is how to interpret signals incoming at various directions and times. One such method used in SONAR systems is phase differencing. Phase differencing works by detecting phase differences between incoming signals received by adjacent receivers. The measured phase difference is then used to determine error in each received signal, allowing the apparent angle of a target detected by the array to be found accurately. A visualization of phase differences between backscatter signals is shown below in Figure 8.

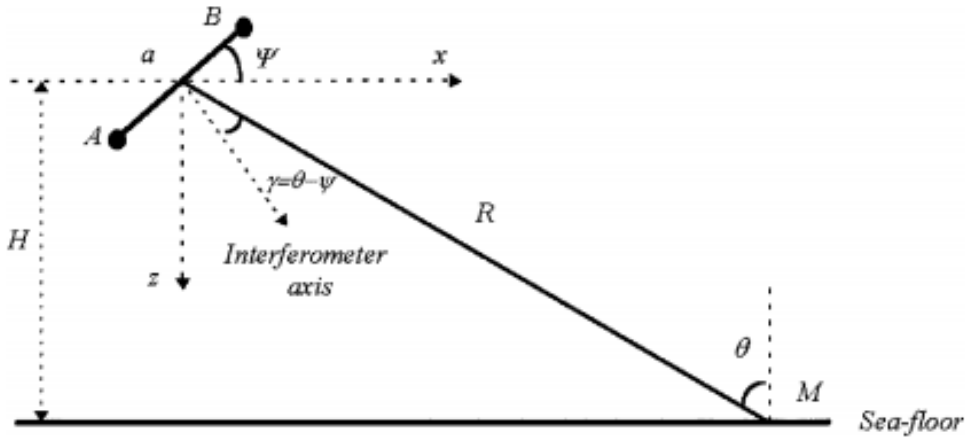

Figure 8. Phase difference visualization (Lurton, 2000)

Points A and B in Figure 8 represent identical line arrays, which applied to this project, would be considered two adjacent quadrants of transducers, with spacing of

length a between them. The measured phase difference of a backscatter signal received from an incident target is defined by the Equation 26.

$$\Delta\phi_{AB} = \frac{2\pi \text{ a } \sin(\gamma)}{\lambda} \qquad \text{Equation 26.}$$

The apparent target angle is defined as θ – ψ and shown in Equation 27.

$$\theta - \psi = \arcsin\left(\frac{\lambda\, \Delta\phi_{AB}}{2\pi\, a}\right) \qquad \text{Equation 27}$$

Solving Equation 27 for θ and differentiating, results in the angle measurement precision as defined in Equation 28.

$$\delta\theta = \frac{\delta\Delta\phi_{AB}}{2\pi}\frac{\lambda}{a}\frac{1}{\cos(\theta - \psi)} \qquad \text{Equation 28}$$

Looking at this equation, the phase different precision is defined as $\delta\Delta\phi_{AB}$, which is proportional to the angle error. It should also be noted that the angle measurement precision is kept small when the spacing is large compared to a wavelength, and when the incident target is closer to the interferometer axis. From this, the depth measurement precision is defined as shown in Equation 29.

$$\frac{\delta z}{z} = \tan\theta\, \delta\theta = \frac{\delta\Delta\phi_{AB}}{2\pi}\frac{\lambda}{a}\frac{tan\theta}{\cos(\theta - \psi)} \qquad \text{Equation 29}$$

Equation 29 shows that as the incident angle of the target becomes larger, the error becomes larger, as more of the signal will be reflected and will not be read by the receiver. Acquisition of the phase angle, allows for bathymetric calculations.

IV. Component Design and Development

A tonpilz piezoelectric transducer is used to generate high power sound at low frequencies[2]. The transducer consists of a light head mass, piezoelectric ceramic ring stack, heavy tail mass, and a central bolt. This type of transducer is commonly used for underwater SONAR applications because it can operate as both a transmitter and receiver. (Massa)

The transducer can be modeled as a spring-mass-damper system. The spring of the system consists of a piezoelectric ceramic ring stack. Whenever an electric field is applied to the polarized piezoelectric ceramics, the ring stack will expand and contract. This causes the head mass to vibrate. This vibration pushes the water molecules in front of the head mass closer together which increases the pressure. The molecules then expand as the head mass contracts. This process continues to neighboring molecules resulting in a wave outward from the transducer. When the ceramic ring stack expands and contracts, the tail mass also vibrates. However, the tail mass was designed to be much more massive than the head mass such that the vibration is minimal. The tail mass is only meant to act as an anchor for the system. (Massa)

The spring-mass-damper model of the tonpilz transducer was implemented to design a transducer prototype for the SONAR system. This model was based on an operating frequency of 15 kHz. Equation 30 shows how the mass of the system was calculated where f is the operating frequency and k is the estimated spring stiffness. The spring stiffness was estimated using material properties of the piezoelectric ceramic rings. An arbitrarily chosen number of 5 rings was chosen for the initial design.

$$m = \frac{k}{(2\pi f)^2} \qquad \text{Equation 30}$$

The head mass was designed as a cylinder with a central bolt that went partway through the cylinder height. Aluminum 6061 was chosen for the head mass as it is light, easy to machine, and corrosive resistant. With this design and the desired mass of the system, Equation 31 was used to calculate the height of the head mass where ρ_a is the density of aluminum, r_{HM} is the radius of the head mass, r_s is the diameter of the central bolt, and D_s is the depth of the bolt hole. The radius of the head mass must be less than half the signal wavelength to satisfy the spatial aspect of the nyquest sampling frequency.

$$H_{HM} = \frac{m + \rho_a \pi {r_s}^2 D_s}{\rho_a \pi {r_{HM}}^2} \qquad \text{Equation 31}$$

[2] The term tonpilz comes from the German language and is translated directly to mean *tone mushroom*. A tonpilz transducer is so named because of its size and acoustic projection. (Wilson, 1988)

The tail mass was designed to be 4 times more massive than the head mass. This ensures that the vibrations in the tail mass will be minimal and the spring-mass-damper system model holds. To prevent the tail mass from being large, it was made of cold rolled steel. This is much denser than aluminum and easy to machine relative to other steels. The diameter of the tail mass was set equal to the head mass, and the resulting height of the tail mass was calculated.

A transducer prototype was manufactured and assembled. Figure 9 shows the transducer prototype. The aluminum head mass is on the top followed by the ceramic ring stack. Between each of the ceramics are copper mesh rings. Red and black wires are connected alternatively to the copper mesh between each ceramic ring. The red and black wires are then connected appropriately to the function generator. This is how the electric field is applied that makes the ceramics expand and contract.

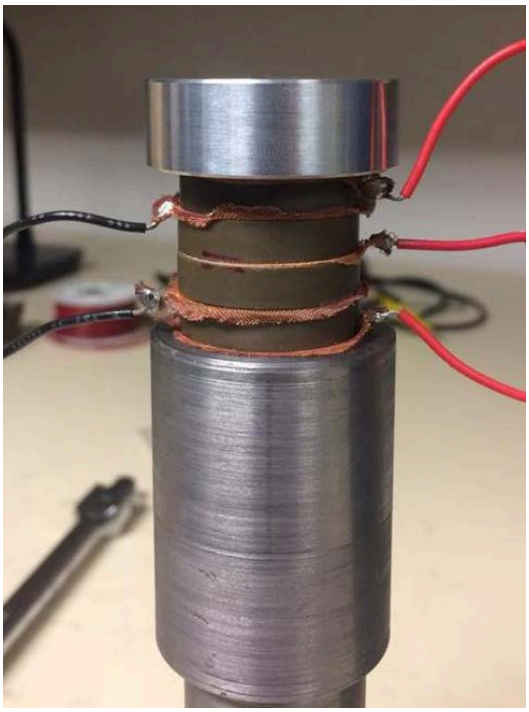

Figure 9. Transducer prototype

Testing on the first prototype was competed to determine the natural frequency of the transducer. Figure 10 shows the experimental set up used to find the natural frequency of the transducer. In this figure, channel 0 and 1 refer to channels on National Instruments DAQ board. The function generator was set to a sweep of frequencies and the measured voltage drop across the resistor.

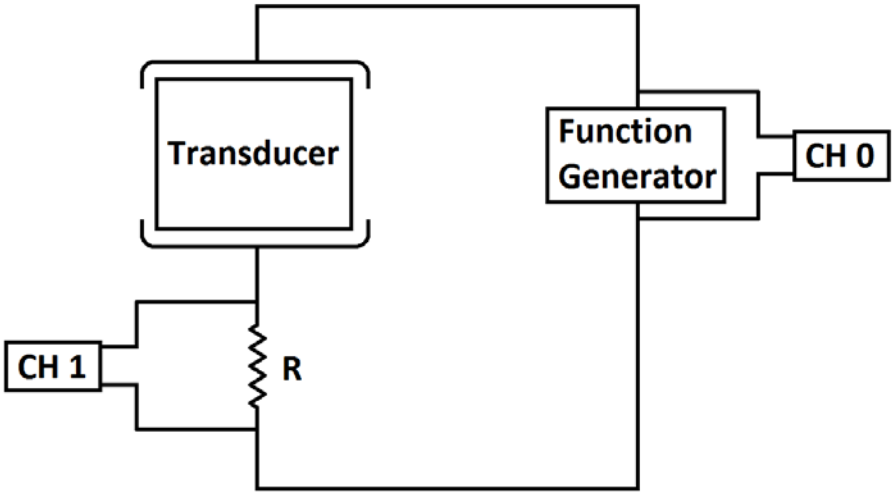

Figure 10. The experimental set up to test the transducer natural frequency

The natural frequency of this prototype transducer was 12 kHz, 3 kHz less than the desired frequency. When creating the initial prototype, the spring stiffness coefficient of the ceramic rings was estimated using material properties. Using the measured natural frequency and the mass of the head mass, an experimental value for the spring stiffness was obtained. Equation ___ shows this calculation and the result. This spring stiffness was used to better predict the desired mass of the system.

$$k = m(\omega_n)^2 = 4 * 10^8 \frac{N}{m} \qquad \text{Equation 32}$$

The head and tail masses from this transducer were utilized to test the effect of different variables on the natural frequency of the transducer. Testing was completed to see how the system changed between 4, 5, and 6 ceramic rings. As expected, additional ceramic rings decreased the spring stiffness thus decreasing the natural frequency. The torque on the central bolt was tested over a wide range. This testing showed that adjusting the torque on the bolt could effectively increase or decrease the natural frequency by approximately 1 kHz. Furthermore, spring washers were added to the central bolt to mitigate the effect of the bolt on the spring stiffness of the system.

With this testing compete and the experimentally determined spring stiffness, the second prototype was design and manufactured. The second transducer design contained the following materials:

- 1 ½ inch diameter aluminum head mass
- 1 ½ inch diameter steel tail mass
- 190 kHz piezoelectric ceramic rings (4)
- Copper mesh rings (5)
- Stainless steel cap screw
- ¼ inch spring washers (6)

Figure 11 shows each of the materials used in the transducer. This picture shows materials required for assembly that are not list above. This includes Teflon tape, electrical tape, and wire. The Teflon and electric tape were used to electrically isolate the ceramic rings and copper mesh from the rest of the system. The wire was soldered to the copper mesh rings to connect the piezoelectric ceramics.

Figure 11. Transducer materials

The second prototype was tested in water to find the impedance, natural frequency, transmit voltage response, and receive sensitivity of the transducer. To do this, a waterproof pot was designed and constructed as shown in Figure 12. In this picture, the transducer is mounted to the flat portion of the white PVC end cap and the pot is filled with non-conductive castor oil. The speed of sound in castor oil is the same as that of water. The end of the pot is covered by a 0.05-inch-thick latex sheet through which the sound waves can pass without attenuation. The pot was mounted to a carbon fiber rod and lowered into the water in the engineering tank in the Chase Ocean Engineering Laboratory.

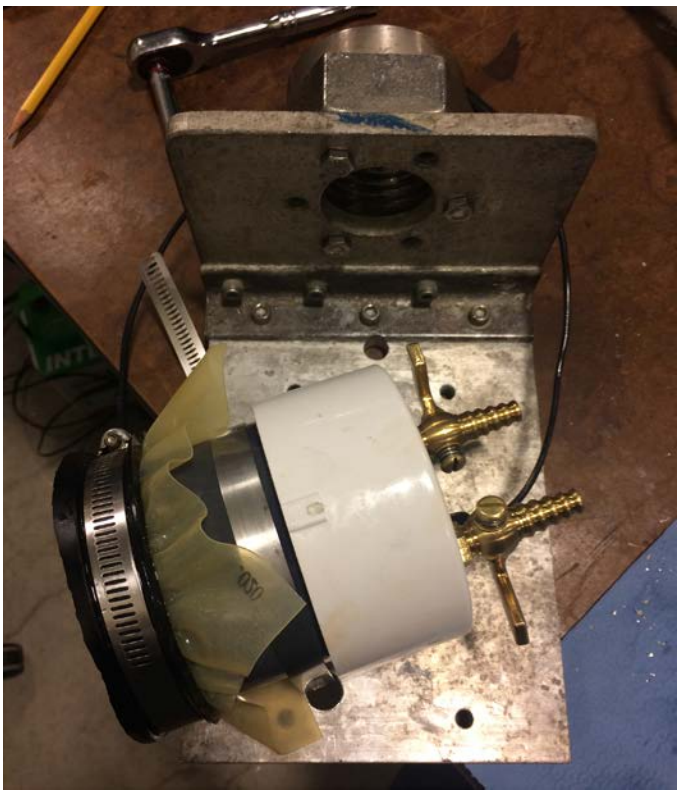

Figure 12. Waterproof pot for individual transducer testing

The transducer was connected to the experimental set up shown above in Figure 12. The outputs of channel 0 and channel 1 of the DAQ are defined as E_o and E_1, respectively. The outputs E_o and E_1 on the DAQ board are not in phase. To correct for this, a phase adjusted value of E_1 is calculated using Equation 33 where φ is the phase shift calculated using the sampling frequency and time constant.

$$E_2 = \frac{E_1}{e^{j\cdot\varphi}} \qquad \text{Equation 33}$$

The voltage drop across the resistor was used to find the impedance curves of the transducer for a sweep of frequencies. The impedance, Z, is calculated using Equation 34 where R is the resistance used in the experimental setup. The conductance, one of the impedance curves, is the real part of the inverse of the impedance. This is shown in Equation 35.

$$Z = \frac{E_o - E_2}{R} \qquad \text{Equation 34}$$

$$Conductance = Re\left\{\frac{1}{Z}\right\} \qquad \text{Equation 35}$$

Figure 13 shows the conductance curve for the individual transducer in water. The natural frequency of the transducer occurs at the peak of the conductance curve. This curve has a peak amplitude at a frequency of 15.75 kHz. This value closely resembles

the desired natural frequency of system of 15 kHz. The peak is relatively wide which suggest that there will be a band of high transmit voltage response and receive sensitivity around this frequency. The width of the peak is a result of the damping of the transducer due to the oil inside the pot.

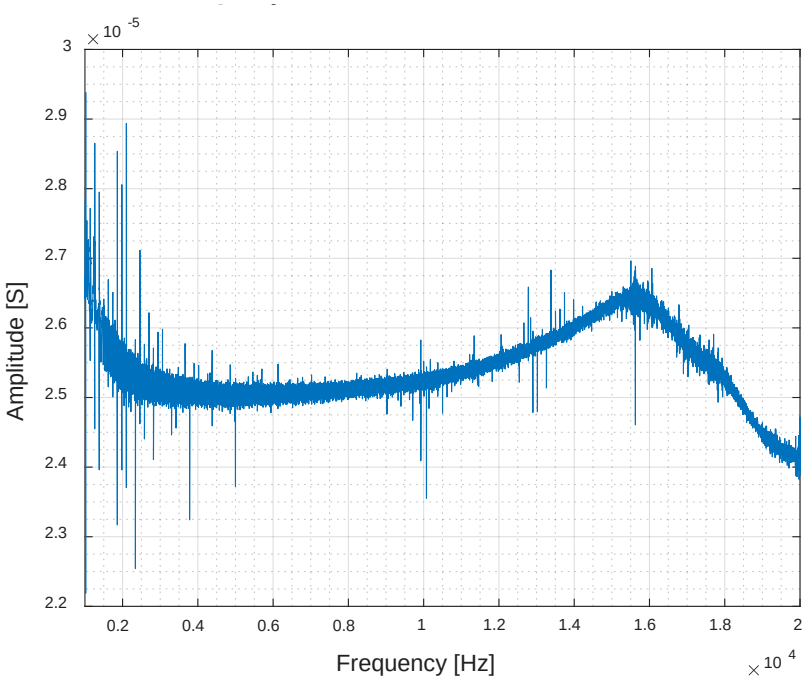

Figure 13. Individual transducer conductance vs. frequency

To test the transmit voltage response and receive sensitivity of the transducer, a RESON TC4034 hydrophone was placed in the water. The hydrophone was placed at the same depth as the transducer and approximately 1.04 meters away. The experimental set-up is shown below in Figure 14. The hydrophone specification sheet can be found in Appendix B.

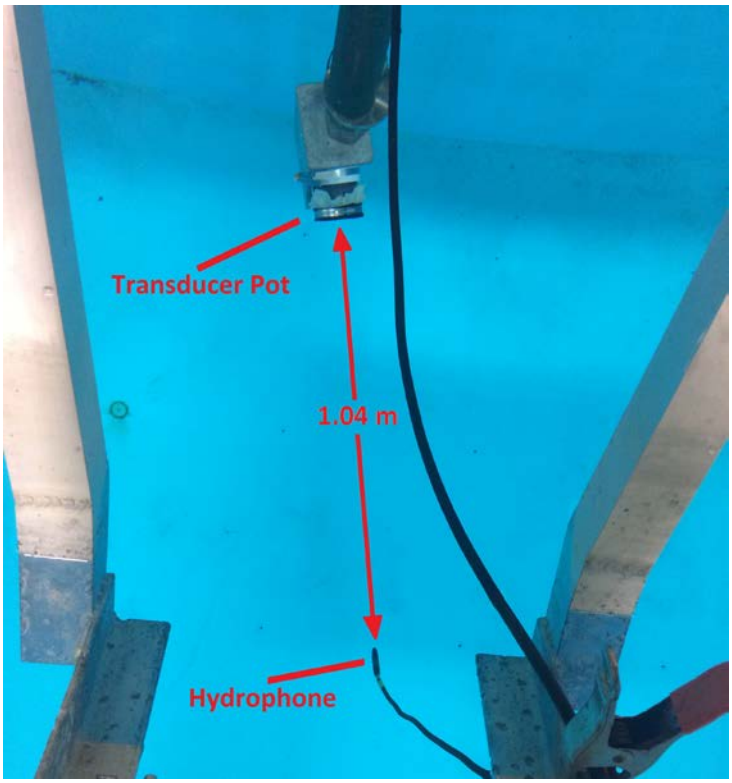

Figure 14. Individual transducer experimental setup

Figure 15 shows the experimental set-up used to collect data for the transmit voltage response (TVR) analysis. The function generator put a sine wave burst to the power amplifier which sent the signal to the transducer. The transducer generated a sound which was read by the hydrophone. This response was put through a pre-amplifier and read by the oscilloscope. The TVR data was collected by recording the amplitude of the root mean square hydrophone voltage on the oscilloscope for a range of frequencies.

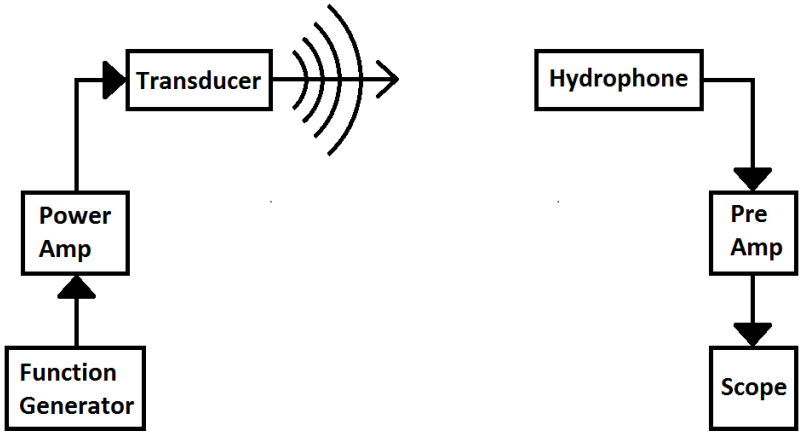

Figure 15. Transmit voltage response experimental setup

The TVR is determined using Equation 36 where V_{drive} is the system drive voltage and SL is the source level. This equation comes from the SONAR equation discussed in Section III of this report.

$$TVR(f) = SL - 20\log_{10} V_{drive} \qquad \text{Equation 36}$$

The TVR versus frequency curve is shown in Figure 16. The TVR is highest in the range of 16.5 to 19 kHz, signifying the transmit bandwidth. The TVR is at 16.5 kHz, which is close to the natural frequency of the transducer. The bandwidth of high TVR is expected because of the width of the peak shown in Figure 16.

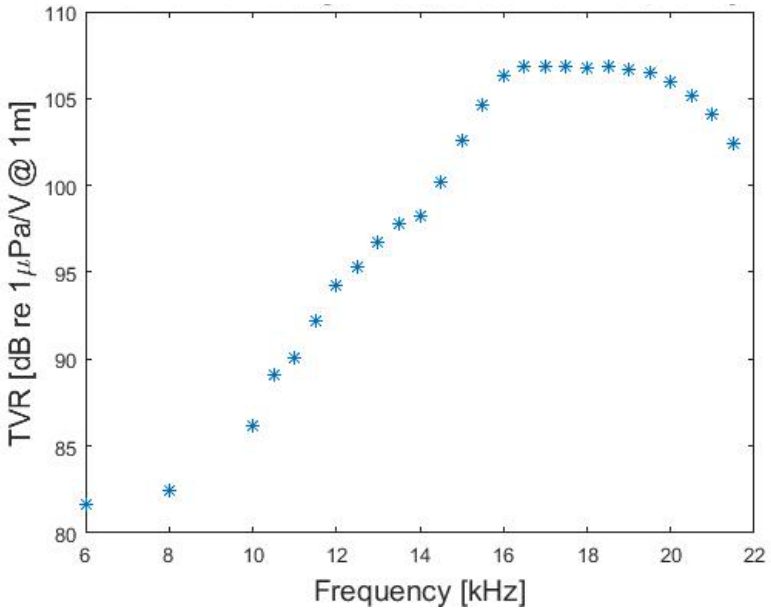

Figure 16. Individual transducer transmit voltage response vs. frequency

The experimental set-up was adjusted to record data for the receive sensitivity (RS) analysis as shown in Figure 17. In this setup, the hydrophone sends the signal which the transducer is receives.

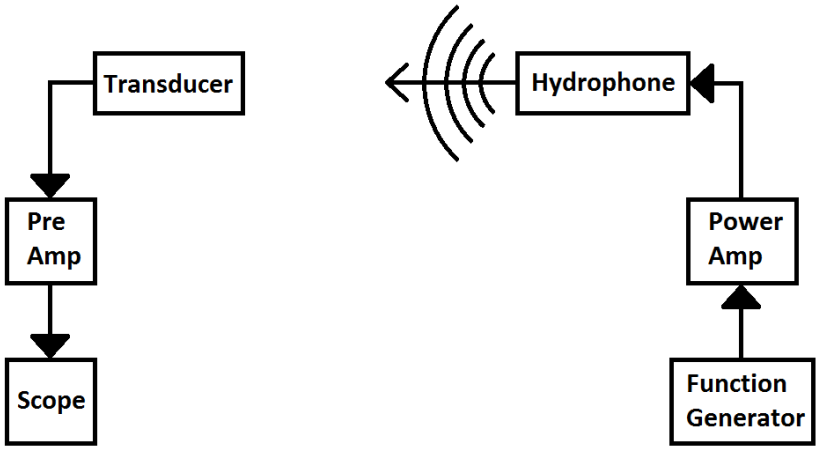

Figure 17. Receive sensitivity experimental setup

The RS of the transducer is calculated using Equation 37 where V is the RMS output voltage of the transducer read on the oscilloscope, G is the gain of the pre-amplifier, and SPL is the sound pressure level. This equation comes from the SONAR equation.

$$RS(f) = 20\log_{10} V - 20\log_{10} G - SPL \qquad \text{Equation 37}$$

The RS results are shown for a range of frequencies in Figure 18. The peak RS is at a frequency of 16 kHz, which is close to the natural frequency of the transducer. The RS should be maximum at the operating frequency of the system to obtain good results when using the transducer for practical application.

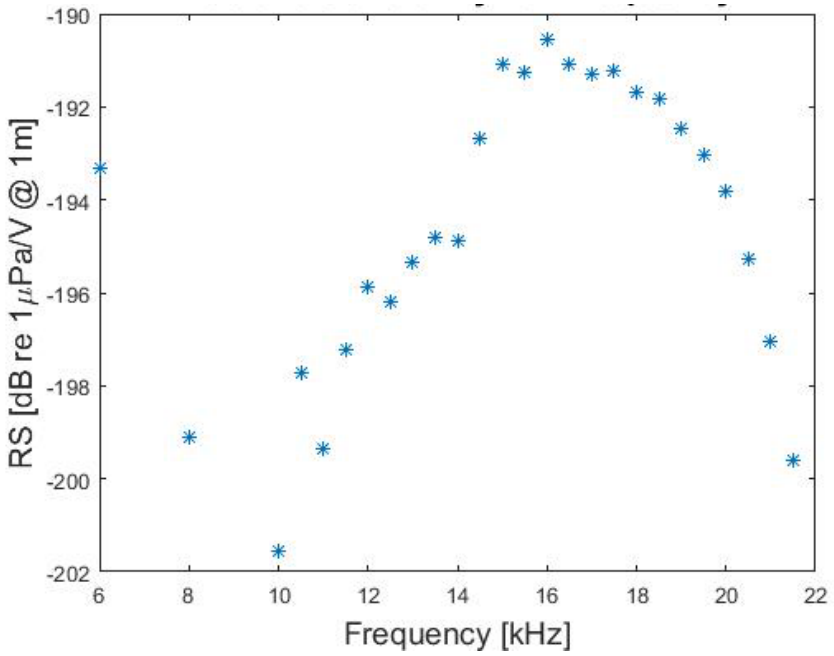

Figure 18. Individual transducer receive sensitivity vs frequency

Based on the results from the impedance, transmit voltage response, and receive sensitivity tests, the final transducer design was chosen. Fifty-two transducer head and tail masses were manufactured in the University of New Hampshire Machine Shop. The number of transducers was chosen based on multiple factors. The SONAR system operates in four quadrants thus the number of transducers must be divisible by 4. In addition, the number of transducers directly affects the width of the beam path. The longer the transducer row is, the narrower the beam path. This results in higher resolution. Lastly, one of the goals of this system is portability. The greater the number of transducers, the heavier and bigger the system. Taking these three factors into account (processing, resolution, and size), the optimal number of 52 transducers was chosen.

Once all the head and tail masses were manufactured, the transducers were assembled as described above. Because the transducers operate in water, the ceramic ring stack and wiring must be electrically isolated from the water. This was done by

casting the ceramic ring stack with a polyurethane elastomer. Appendix C contains the urethane material data sheets. To cast the ceramic ring stack in urethane, a silicone mold was made that fit around the transducers. Pictures of the silicone mold are shown below in Figure 19 and the material data sheet can be found in Appendix D. The process to create the silicone molds is described in Appendix E.

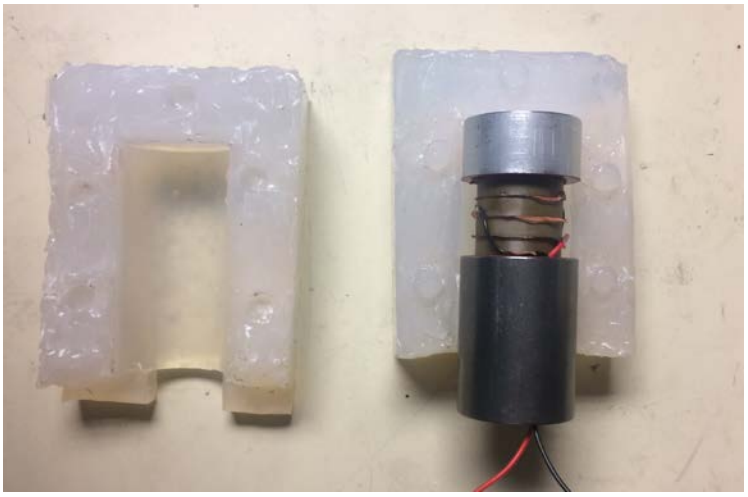

Figure 19. Transducer inside silicone mold

The urethane casting process is detailed in Appendix F and a completed transducer is shown in Figure 20. The urethane casting was initially done for 3 test transducers. The test transducers were tuned to frequencies of 14.5, 15.5 and 16.5 kHz prior to casting in urethane. Regardless of the starting frequency, the casted transducers had a resulting frequency of about 16.5 kHz. This may be a result of the pressure (55 psi) used in the pressure chamber during the casting process. Because of the resources available and time, it was decided that the SONAR system would operate at 16 kHz. This is within 1.5 kHz of the goal frequency, 15 kHz. This has a slight effect on the system parameters regarding the swath limit. However, the system can still achieve the goals of this project at an operating frequency of 16 kHz.

Figure 20. Transducer casted in urethane

With the urethane casting complete, an individual transducer was once again placed in the Chase Ocean Engineering Tank for testing. The TVR and RS results are shown below as Figure 21 and 22, respectively. Both the TVR and RS have peaks of acceptable amplitude near the operating frequency of the system.

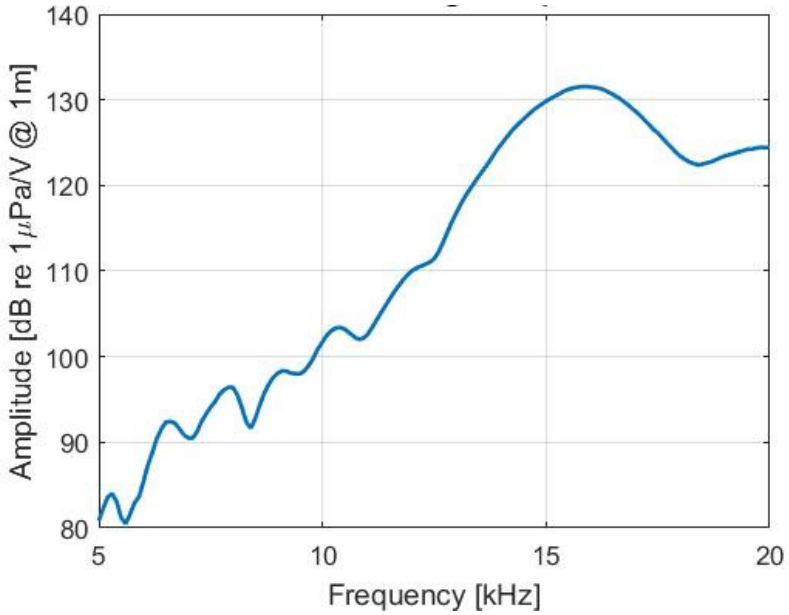

Figure 21. Casted transducer transmit voltage response vs. frequency

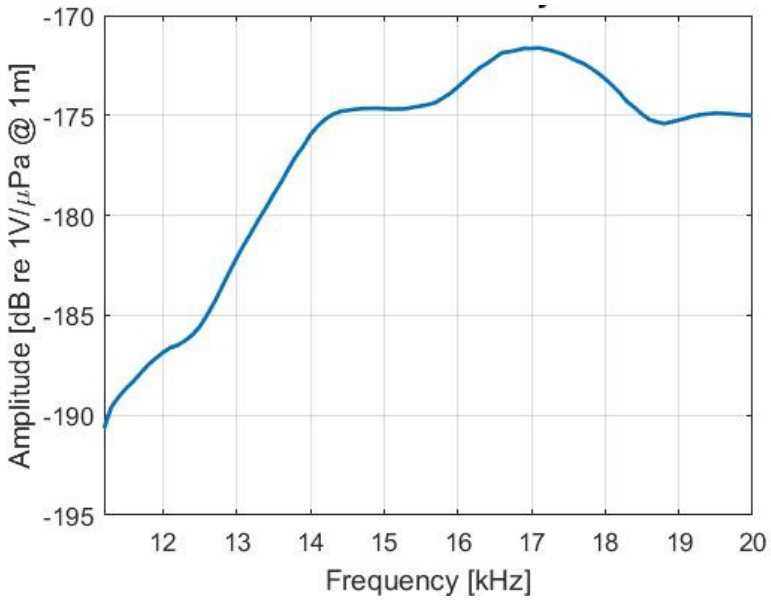

Figure 22. Casted transducer receive sensitivity vs. frequency

The transmitting beam pattern for the individual casted transducer was also tested and the results are shown in Figure 23. An explanation of beam pattern can be found in Section III of this report. The results are not symmetrical about 0°. This suggests that the head mass is not symmetrically constrained and vibrating around the center of the transducer. However, the peak bandwidth of the beam pattern is around 0°, which is desired.

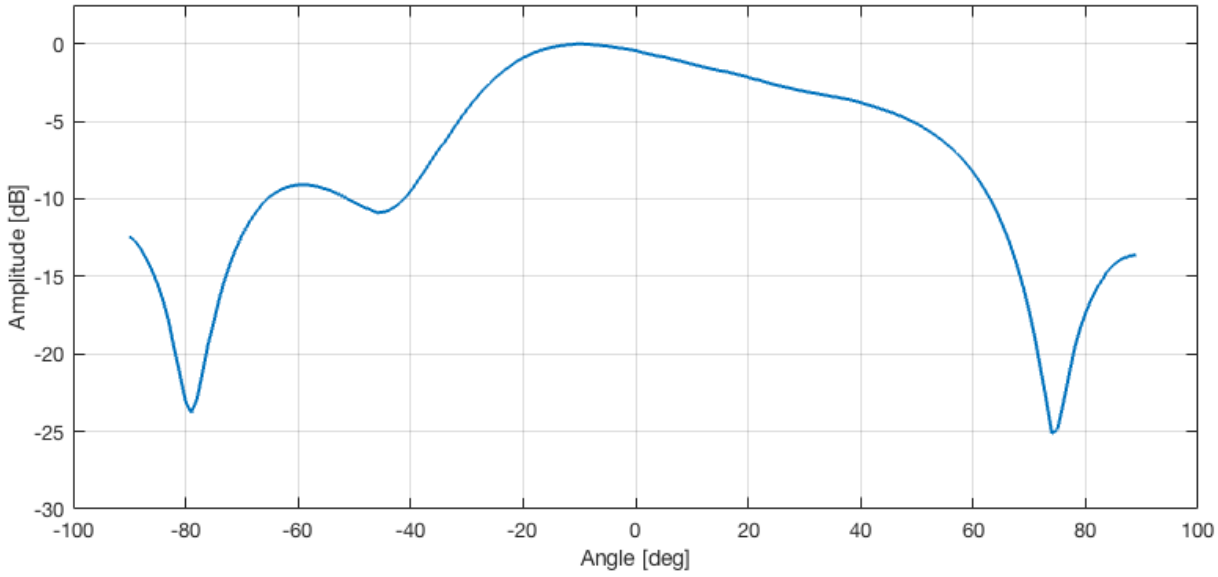

Figure 23. Casted transducer transmitting beam pattern

With acceptable results for TVR, RS, and transmitting beam pattern, the remaining transducers were casted in urethane. The tail mass on each transducer was painted

with *Rust-Oleum* for protection from the tank and sea water. This completed the assembly off all 52 transducers.

Prior to mounting the transducers to the stave, each was tested for electrical isolation. The transducers were designed so that the tail and head mass were electrically isolated using electrical tape. In testing, it was found that the method used to electrically isolate the transducers was not successfully. The black wire in the transducer was electrically connected to the tail and head mass. Although this is not ideal, the system can still operate so long as the black wires from each transducer are connected when assembling the system.

V. System Assembly

To utilize the transducers in the SONAR system, it is necessary to both design and manufacture a stave[3]. The stave is a fixture which the transducers can be mounted to. A SOLIDWORKS image of the stave is shown in Figure 24 below.

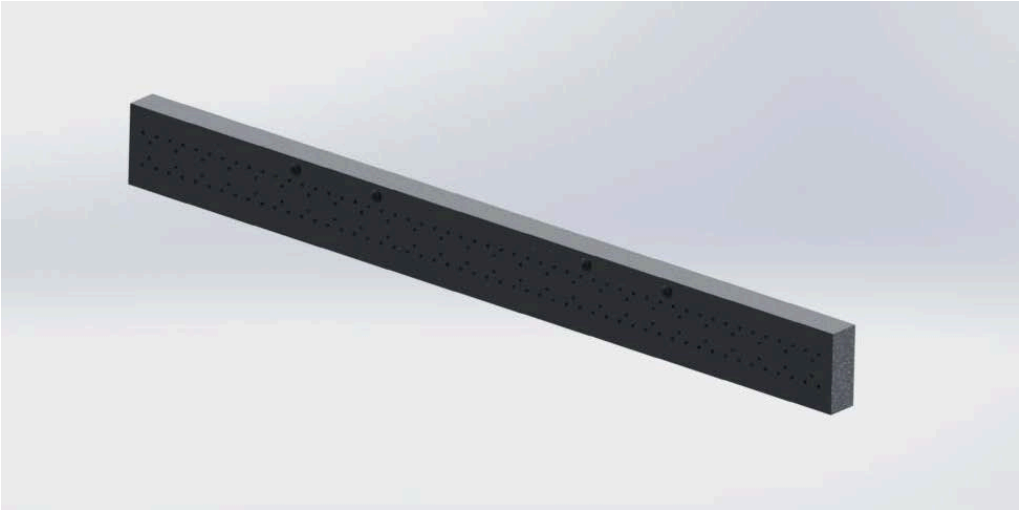

Figure 24 Final Design of Stave

While designing the stave several constraints need to be taken into consideration. Because the SONAR system will be tested on the Gulf Surveyor, it must be small enough to fit in the moon well of the Gulf Surveyor. This limits the length of the stave to 2 meters. To keep the stave lightweight it is manufactured out of 6061 aluminum.

In addition to bearing in mind the overall size, it is necessary to insure that in each quadrant none of the transducers are more than half a wavelength apart (a wavelength is defined by both the speed of sound in water and the operating frequency of the transducers). This is found using Equation 38 below, where d is the spacing of the transducers, c is the speed of sound in water and f is the operating frequency of the SONAR system.

$$d = \frac{c}{2f} \qquad \text{Equation 38}$$

This value is found to be 50mm. This is necessary for the system to be able to measure phase differences in the return signal. Likewise, it is necessary to ensure that the two rows of transducers are no more than half a wavelength apart.

Once the overall dimensions have been determined using the physical constraints, it is necessary to determine how the transducers will be mounted to the stave. Each

[3] Stave, translated directly, means a vertical wooden post or plank in a building or other structure

transducer is designed with two tapped holes opposite of each other as well as a hole through which the wiring can pass through. As a result, three through holes are machined into the stave for each transducer. This allows two screws to pass through the back of the stave and thread into the rear of the transducers. This also allows the wiring to pass from the rear of the tail mass to the back of the stave.

To isolate the wiring in the back from the water, a series of four channels are created and shown in the SOLIDWORKS image in Figure 25 below.

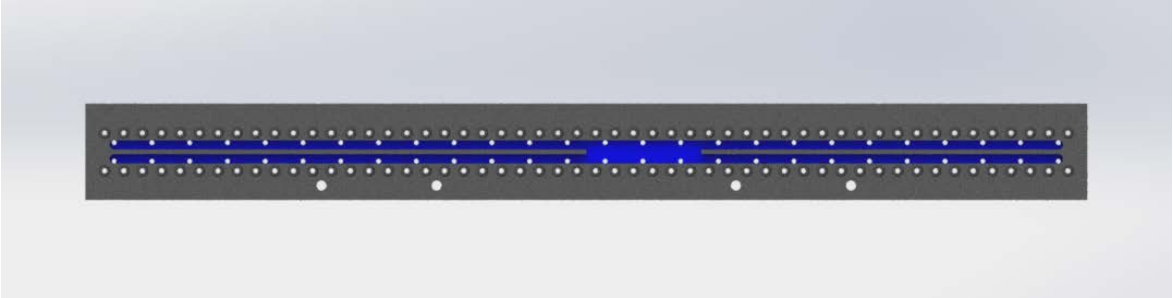

Figure 25 Channels in the Back of the Stave

The wires for each quadrant are separated into each of the channels and wired in parallel. The wires from each quadrant are then joined in the center of the stave by an inline underwater 10 pin cable connector. The connector is used during both tank and field testing to route all the wiring in the SONAR system to the instruments in the UNH acoustic testing tank and the Gulf Surveyor. After the wiring is completed the channels are filled in with polyurethane. A SOLIDWORKS image of the final design can be seen below in Figure 26.

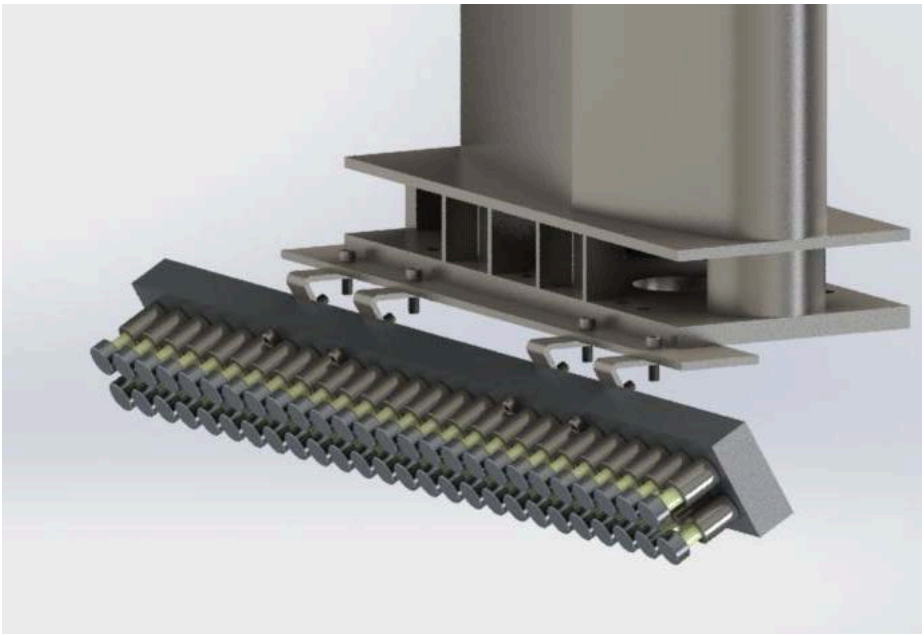

Figure 26 Assembled SONAR System mounted on Gulf Surveyor

To mount the stave to the Gulf Surveyor, an adapter plate is designed. The adaptor plate is manufactured from a steel plate to ensure that it will be strong enough to hold the entire weight of the SONAR system. A SOLIDWORKS image of the adaptor plate is shown in Figure 27.

Figure 27 Adaptor Plate

A series of holes are machined into the plate on one side to match those found on the mount of the Gulf Surveyor and the mount of the UNH acoustic testing tank. On the other side of the plate, a series of 4 holes are machined. These allow the stave to be bolted to the adapter plate using a set of 4 angled brackets.

After the stave has been manufactured and the transducers have been attached, testing of the entire system was done in the Chase Ocean Engineering tank. It is found that shortly after placing the SONAR system in the tank that the transducers are not waterproofed. This has caused extensive setbacks in the project.

To remedy this issue, the water first needs to be removed from the SONAR system. To remove the water, a large vacuum chamber is created using PVC piping. The entire SONAR system is placed in the assembly and placed under vacuum. A heat lamp is directed toward the vacuum to heat it. This causes the water to evaporate and exit the transducers in the SONAR system. Water is successfully removed from two of the four quadrants using these methods. The remaining two quadrants are permanently damaged and are unable to be used during testing.

This process is repeated multiple times until the system is completely waterproofed. After drying the system out, epoxy is poured over the top of the stave, around the individual transducers, to completely seal the small gap between the rear of the transducers and the stave. All holes in the back of the stave are also filled with epoxy to keep water from leaking through the rear of the transducer.

Once the system has been effectively water proofed the SONAR system is ready for field testing.

VI. Electronic Design and Development

The SONAR electronics consist of transmit and receive circuitry. The transmit circuit includes a signal generator, power amplifier, and transformer, shown in Figure 28. The receive circuit uses a LT1125 quad operational amplifier which is shown in Figure 29. Design of the circuits followed a similar process as the transducers design in that the circuits are first simulated using software before being built. A general circuit design outline is found in the book "The Art of Electronics" by Paul Horowitz (Horowitz, 2015). This design is simulated using NI Multisim [4]. The actual amplification values needed for transmit and receive circuits are not known until tank testing of a transducer is completed. The circuit simulation provides a proof of concept and allows for the parts to be ordered. These parts are implemented once parameters are better defined through testing of the transducers.

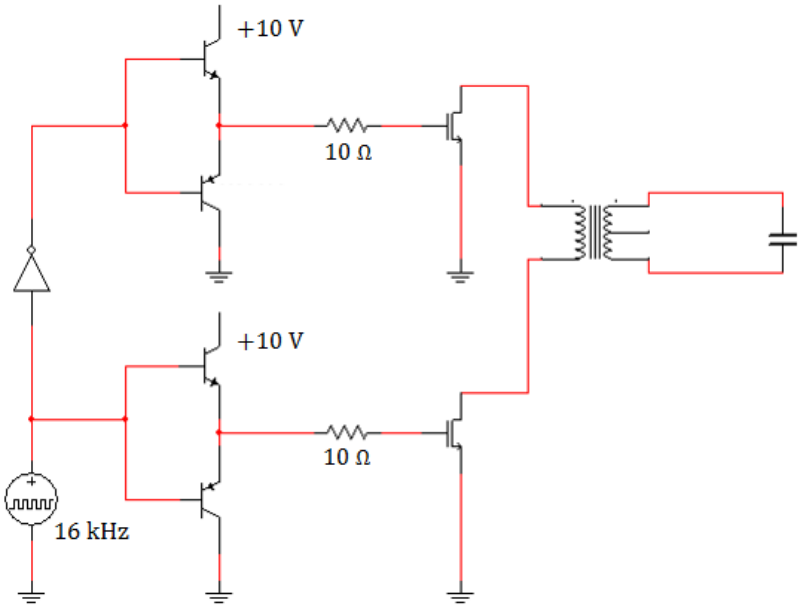

Figure 28 The transmit circuit (Horowitz, 2015)

[4] NI Multisim is an electronic simulation program used to design circuits.

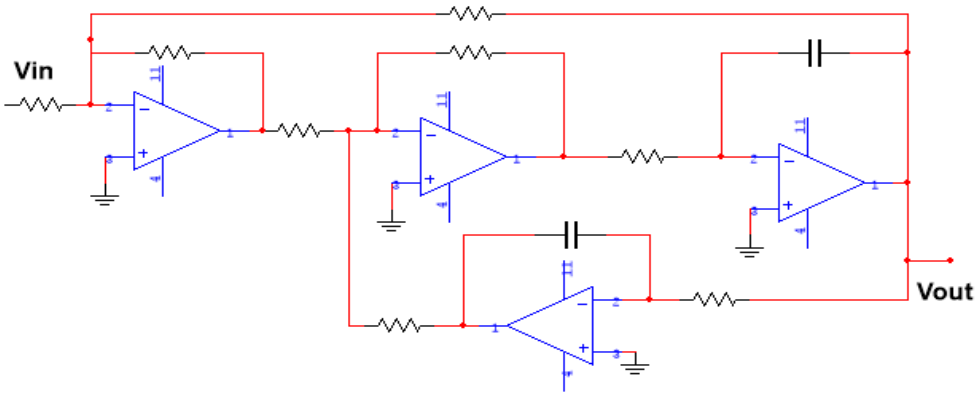

Figure 29 The receive circuit (Horowitz, 2015)

Once tank testing on an individual transducer is completed, the data gathered is analyzed in MATALB and the values required for the power amplifier and receive circuit are determined. On the transmit side, in order for the signal to be received in 20-100 meters of water, the power amplifier needs to deliverer 200W of power to the transducers. On the receive side, the transducers were found to be so sensitive that no amplification is required. For the expected water depths that occur in Portsmouth Harbor during testing (20-100m), the dynamic range of the Analog to Digital converter can convert the incoming analog signals to digital without amplification. This simplifies the receive circuit from a filtering and amplification stage to just a filtering stage. The goal of filtering the receive circuit is to only measure values within the range of the transmitted signal, thus filtering out excess noise from the boat and ocean. The filtering on the receive side is performed by the quad op amp, which serves as a bandpass filter from 15-17 kHz. A schematic of the transmit and receive circuits is shown in Figure 30 below.

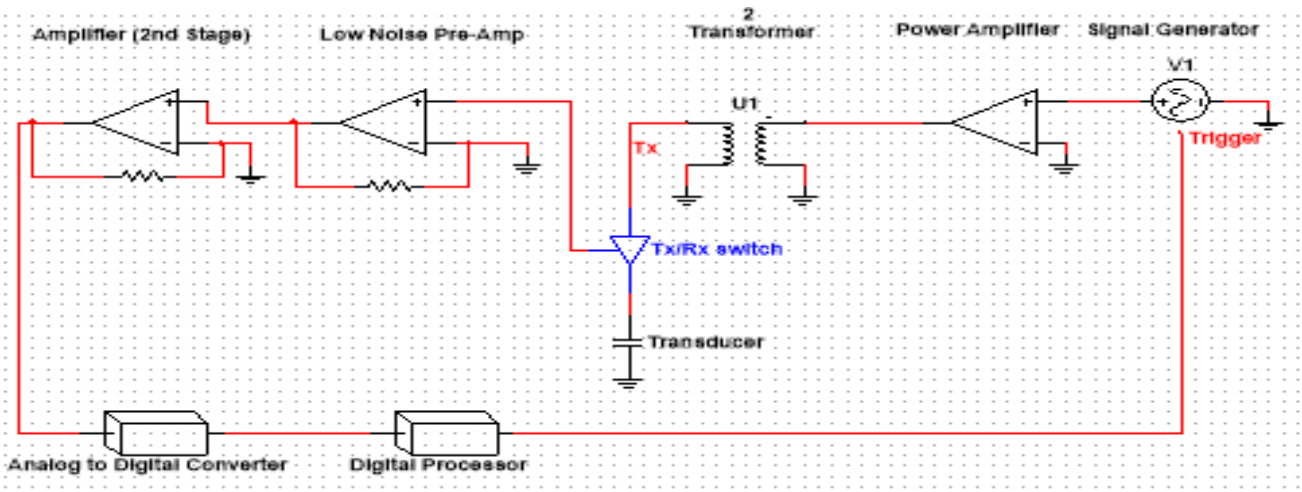

Figure 30: Circuit diagram for the SONAR

The electrical components are implemented so that they can be replaced with more advanced components when needed. At deeper water depths the reflection of acoustic energy from a continuous wave signal at depth may not be strong enough to register, therefore the continuous wave signal will be replaced with a CHIRP signal. This CHIRP signal will help elevate the transmitted pulse above the noise floor. Adding amplification to the receive circuitry will also occur by changing resistor values. A signal generator is used to create a waveform that is sent to the transducers. Future design considerations will use a chip based solution that will be more compact and cost effective then a signal generator.

VII. Signal Processing

The SONAR system requires powerful data acquisition hardware. When operating the system, a frequency chirp is sent to the transducers which act in parallel to output a strong signal. All quadrants are then switched to listening mode to gather the incoming signal. The system measures the return signal in each quadrant separately at a high sampling rate. A higher sampling rate increases frequency resolution as denoted by Equation 39. However, there is a tradeoff between temporal resolution and frequency resolution. If the sampling rate is fixed, the resolution is determined by the number of samples, N. Frequency resolution is important for filtering out unwanted noise during signal processing.

$$\Delta f = \frac{1}{t} = \frac{f_s}{N} \qquad \text{Equation 39}$$

Custom data acquisition hardware was one of the goals of the Poseidon Project. The goal was to eliminate system dependence on expensive industrial equipment, furthering financial accessibility. The SONAR system requires four channels, one from each quadrant, to be measured accurately at high frequency for usable data. Several microprocessor boards were considered for data acquisition. The Arduino Due was chosen for its relatively high clock speed and built in analog to digital converter. However, several problems arose while working with the Arduino. There is only one analog to digital converter on the board, limiting analog voltage readings. The Arduino has a multiplexor that can route four separate channels to the analog to digital converter, but it needs a significant amount of time to stabilize. This is not ideal when working with a system taking samples at high frequency.

Due to the high data demand, the Simrad EK80 transceiver was used during field testing. The Simrad EK80 is a scientific wide band echo sounder with high dynamic range and low self-noise. The system incorporates real time echo and target strength analysis. During testing, the EK80 sent an 11-18 kHz chirp and collected return data at an 117,190 kHz sampling frequency. A match filter was applied to amplify the return signal.

A spectrogram of one return signal is shown below in Figure 31. The expected return signal, from 11-18 kHz, is seen with a return value from –115 to –90 dB/Hz. Strong noise with a frequency component from 20-22.5 kHz is seen constantly throughout the signal. The noise appears to be systematic; several sources were analyzed.

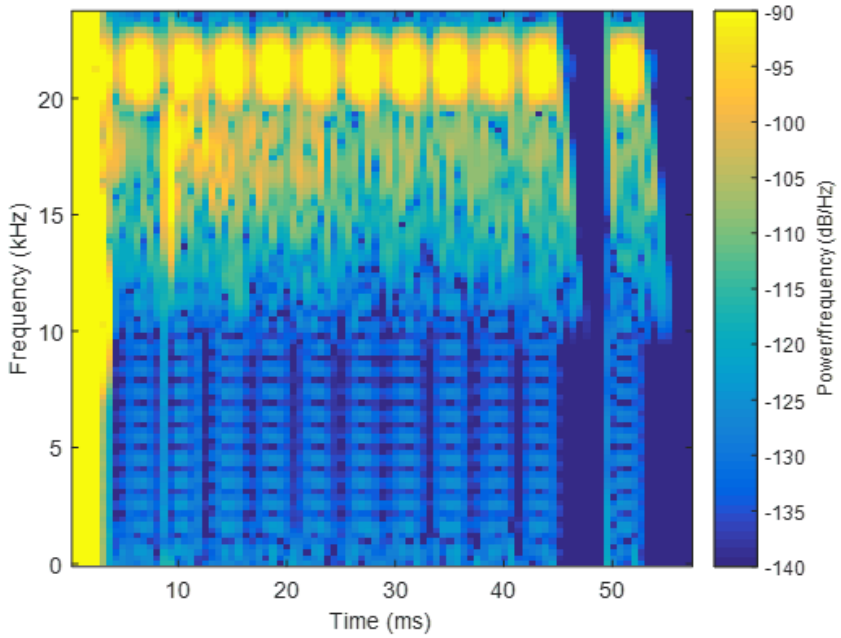

Figure 31: Spectrogram of one ping, strong noise in 20-23 kHz frequency range

Table 5 shows some noise sources that were considered. The operating frequency of the diesel engine onboard the Gulf Surveyor and its electric generator are too low to cause the noise. Even considering 2nd and 3rd mechanical vibration harmonic frequencies does not come close to the frequency of the noise. There is a possibility that the noise is aliasing from a high frequency source, such as a radio station. The transducers were not electrically isolated from the Gulf Surveyors mount. The system assembly could potentially act like a large antenna and magnify strong radio frequencies. The table includes the frequency from a local AM radio station in Dover, NH, which could explain the large frequency spectrum of the noise[5].

Table 5: Possible Noise Sources during the field test

Noise Source	Frequency
Diesel Engine Operating Frequency	43.33 (Hz)
Generator Operating Frequency	60 (Hz)
AC Voltage Supply	60 (Hz)
AM Radio Station	1270 (KHz)

The high end of the backscatter frequency spectrum is very close to the 21 kHz noise. Filtering the noise from the backscatter data required a precise band stop filter. The Butterworth filter is designed to stop frequencies at a specific range with minimal loss to frequency outside of that range. The frequency falloff rate is determined by the order of filter transfer function. A 7th order filter was used, which minimized

[5] AM stations are assigned a 10 kHz frequency

frequency filtering of the desired 11-18 KHz. Figure 32 shows the return signal after applying the Butterworth filter.

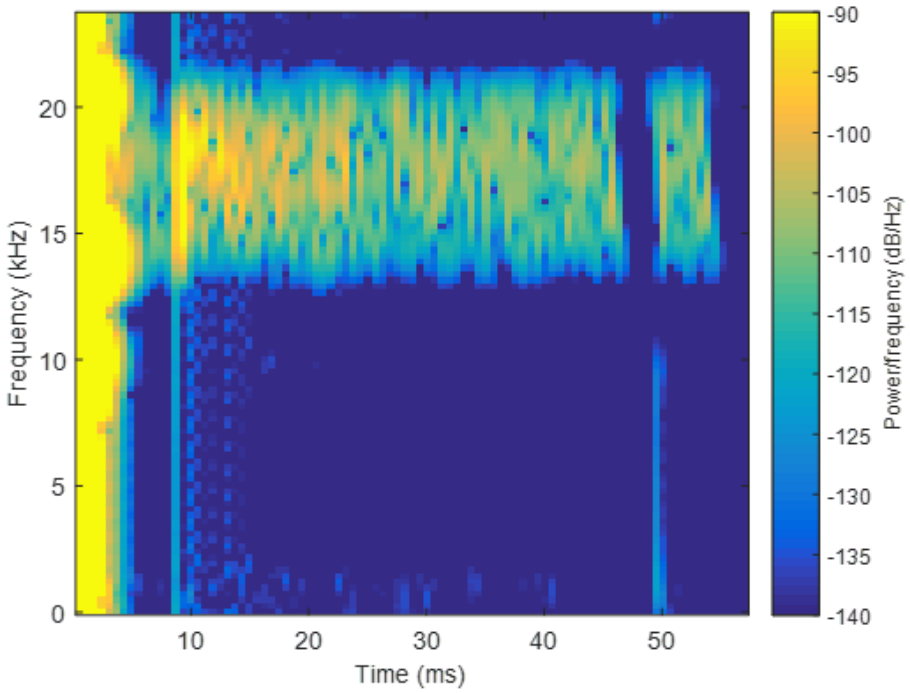

Figure 32: Spectrogram of one ping with the Butterworth filter applied.

The filtered data was used to generate a waterfall plot, shown in Section VIII of this report in Figure 33. The range axis was generated with Equation 40. In this equation, the variable c is the speed of sound in water and was assumed to be a constant 1500m/s. Since the strength of the return signal decreases with distance from transmission loss, the return signal's range dependency was normalized by adding $30\log R$ to account for both the spherical spreading and attenuation loss.

$$R = t * \frac{c}{2} = \frac{N}{F_s} * \frac{c}{2} \qquad \text{Equation 40.}$$

VIII. Results and Discussion

The culmination of this design project was testing on the University of New Hampshire's research vessel, the Gulf Surveyor. The system was installed on the Gulf Surveyor's inertial measuring unit plate and was lowered through the moon pool into the Piscataqua River. All four quadrants of the system were hooked up to the Simrad EK80 transceiver and a signal was sent to the transducers. Using the transceiver software, is was confirmed that sound was being produced by the system. During these initial tests, it was discovered that although steps were taken to fix the electrical shortages that occurred during the first water test, there was still shorting in two quadrants. This is discussed in more detail in Section IV of this report.

Using the backscatter image created in Section IV some conclusion about the riverbed can be made. Figure 33 shows the processed back scatter image. The horizontal axis of Figure 33 corresponds to the ping number which can interpreted as horizontal distance along the riverbed. The vertical axis of Figure 33 corresponds to the distance in meters from the SONAR system. The black space at the top of the image shows how deep the water column is directly underneath the SONAR. As the ping number increase, the contour of the seabed underneath the vessel changes.

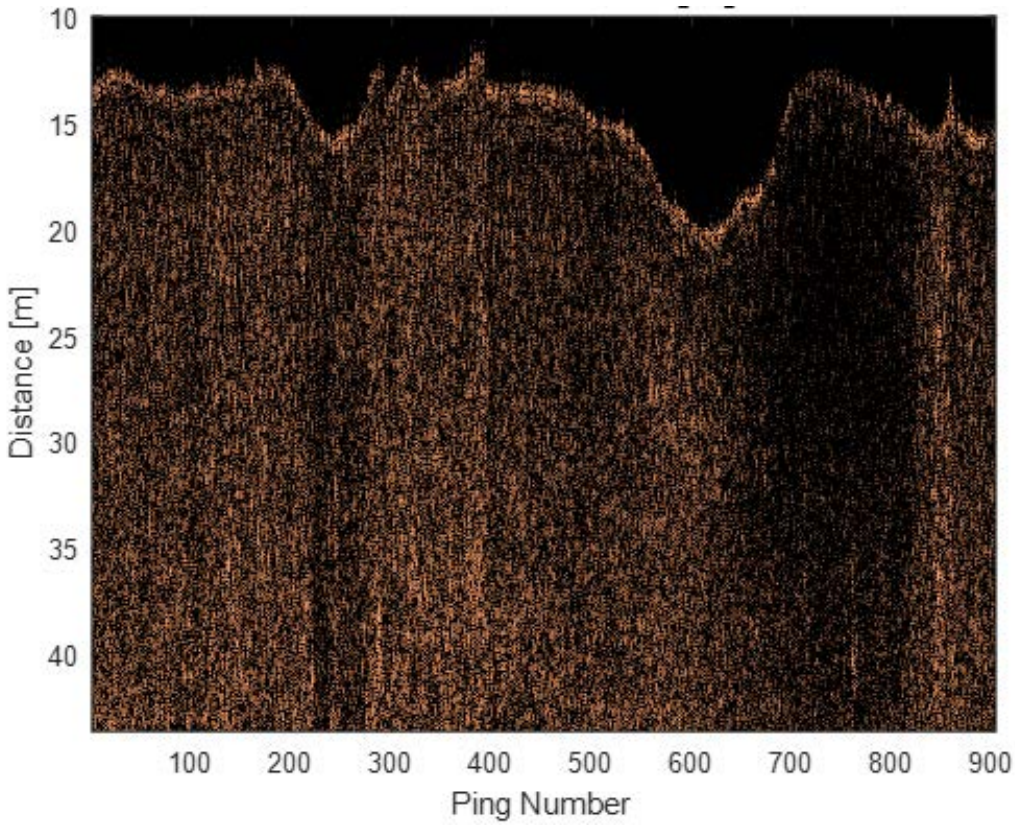

Figure 33. Processed side scan SONAR image

The change in intensity of the backscatter echoes is also seen in the image. The change in intensity helps to depict the target material. Figure 33 highlights different

areas of intensity. Area 1 shows a dark spot which indicates that the seabed has a weak backscatter, this is likely a very fine sand or a clay material. Area 2 has a much stronger backscatter which is an indicator that the seabed has a stronger backscatter, this is likely gravel.

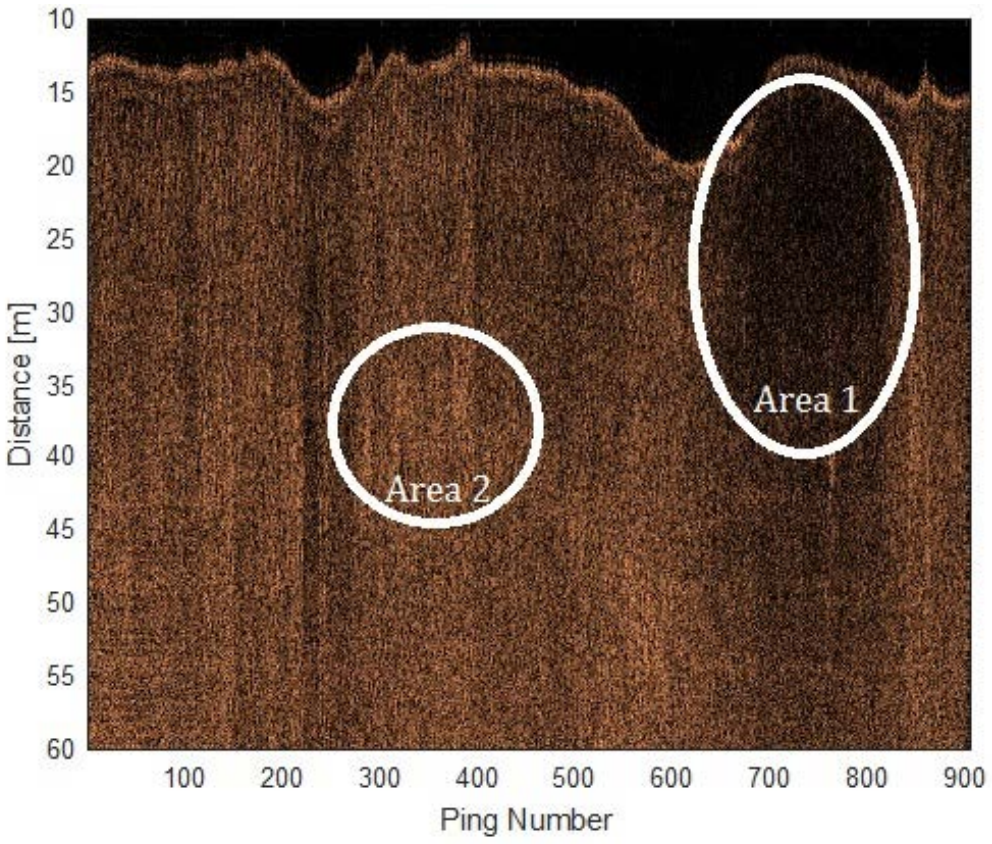

Figure 34. Processed side scan image with areas of interest

The presence of sand waves underneath the vessel is also seen in the SONAR image. In Figure 35 the sand waves have been expanded from Figure 34. Figure 35 shows detail capable of characterizing the sand waves of the seabed. A higher resolution image could be obtained with all four quadrants in operation.

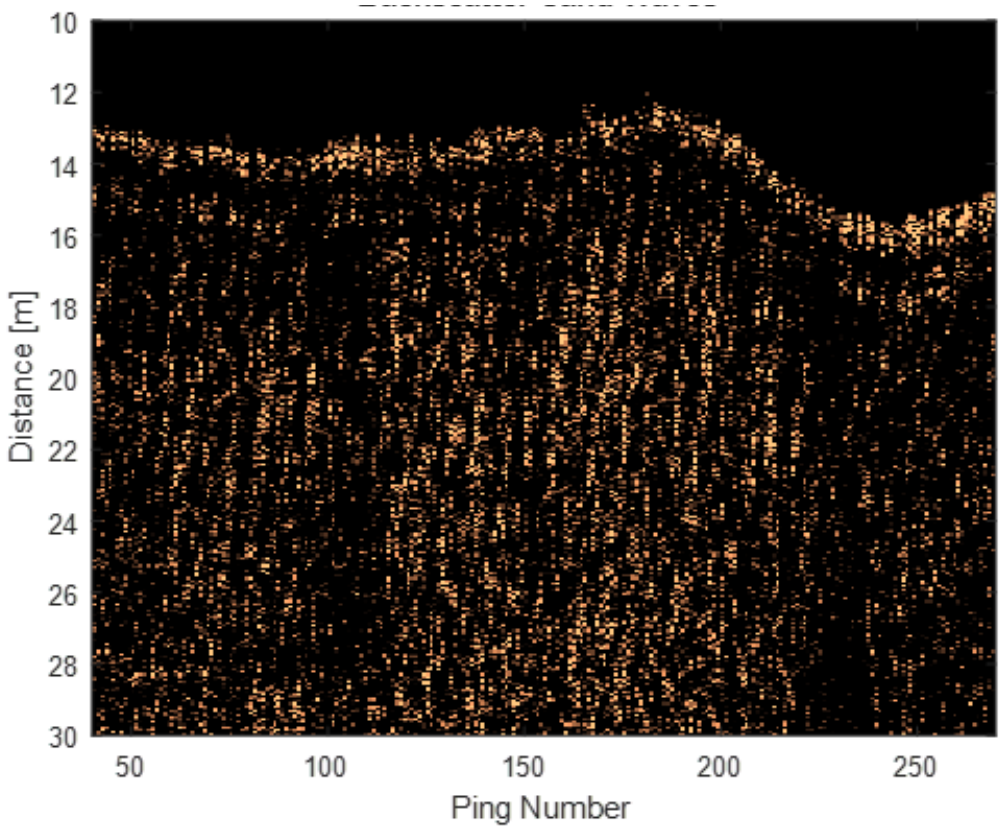

Figure 35. Section view of side scan SONAR image showing sand waves

IX. Conclusion

In its first established year the Poseidon Project has proven a valuable undertaking in the development, fabrication, and testing of this bathymetric side scan SONAR system. As a multifaceted interdisciplinary team, there were many lessons learned that would have not been possible without the involvement of all the different disciplines. These lessons came from many setbacks. The most detrimental of the setbacks was the first attempt at water testing the fully assembled stave. The persistence of pressurized water seep through cracks is detrimental to the system's full operation. In addition, failing to electrically isolate the piezoelectric cells caused excessive noise when recording in a controlled environment such as the harbor testing.

Even though there were setbacks there were many successes and triumphs. The construction of a functional side scan SONAR system, the major goal of this endeavor, was successfully completed with time to test aboard the UNH Gulf Surveyor. The appropriate documentation of specific manufacturing techniques for underwater transducers is now publicly documented for institutional development. This includes documentations of tuning tonpilz transducers and techniques to shape molds for polyurethane casting. With these elements and new levels of understanding the construction of a fully function two swath bathymetric system is possible. The team looks forward to future exploration with UNH into a fully constructed and functional bathymetric SONAR system.

References

Copley, J. (2014, October 4). *Mapping the deep, and the real story behind the "95% unexplored" oceans*. Retrieved from University of South Hampton.

Fin, A. (2010, October 14). *Tapping the Oceans Mineral Wealth With Deep Sea Mining*. Retrieved from OilPrice.com.

Francois, R. E., & Garrison, G. R. (1982). Sound absorption based on ocean measurements: Part II: Boric acid contribution and equation for total absorption. *Journal of the Acoustical Society of America*.

Horowitz, P. (2015). *The Art of Electronics.* New York: Press Syndicate of University of Cambridge.

Israel, B. (2010, June 07). *World's Oceans Remain Largely Mysterious*. Retrieved from LiveScience.

Jackson, D., & Richardson, M. (2011). *High-frequency seafloor acoustics.* New York: Springer.

Kinsler, L., Coppens, A., & Sanders, J. (2000). *Fundamentals of Acoustrics* (Vol. 4). New York: John Wiley & Sons.

Lurton, X. (2000). *Swath Bathymetry Using Phase Difference: Theoretical Analysis of Acoustical Measurement Precision.*

Massa, D. P. (n.d.). *An Overview of Electroacoustic Transducers.* Hingham, MA: Massa Products Corporation.

Side Scan Sonar. (n.d.). Retrieved from NOAA Office of Coast Survey: https://www.nauticalcharts.noaa.gov/hsd/SSS.html

Weber, T. (2017, March). Read Raw Data. Durham, NH: Personal Communication.

What is Sonar? (2014, January 23). Retrieved from NOAA U.S. Department of Commerce: http://oceanservice.noaa.gov/facts/sonar.html

Wilson, O. (1988). *Introduction to Theory and Design of Sonar Transducers.* Peninsula Publishing.

Appendices

A. Budget

Date	Vendor	Cost	Desciption
Design/Prep			
11/21/2016	McMaster-Carr	101.26	Pipe, Pipe cap, wires, Rubber boot, Steel and Aluminum Stock
11/21/2016	Amazon	9.99	cable glands
11/29/2016	McMaster-Carr	46.28	Socket head screws, sealing washers, Square Drive Ball-Point Hex-Bit Socket
12/1/2016	McMaster-Carr	7.77	Nylon Threaded Pipe Fitting
12/1/2016	MSC	41.06	pipe tap
12/7/2016	UPS	10.96	Return of Pipe Tap- Shipping
12/8/2016	MSC	-41.06	return pipe tap
Sub Total		176.26	
Transducer			
1/9/2017	McMaster-Carr	466.87	Steel and Aluminum Stock, Steel Screws
1/10/2017	UPS	65.02	Shipping Return of 304 Steel
1/12/2017	MSC	45.54	Collet
1/15/2017	UPS	-0.42	UPS
1/19/2017	Steminc Piezo USA	1858.55	Ceramic Rings
1/20/2017	Choice Metals	187	Cold Roll Steel
1/23/2017	MSC	38.17	End Mill
1/24/2017	McMaster-Carr	-350.74	Return of 304 Steel
2/8/2017	Assoc Spring Raymo	219.31	Spring Washer
2/8/2017	McMaster-Carr	53.86	Copper Mesh
2/27/2017	Target	14.93	HD plexiglass and glue
2/27/2017	Target	21.16	Target- clay
2/23/2017	Target	17.99	Wire
2/21/2017	BJB Enterprise Inc	290.86	Urethane, color, silicone, rods
Sub Total		2928.1	
Stave			
2/28/2017	McMaster-Carr	367.62	Stave Stock and Plate Stock
3/9/2017	McMaster-Carr	261.47	Screws, Corrosive Resistant Paint, Washers and Angled Connectors
3/22/2017	McMaster-Carr	113.17	Annodes, Paint, Screws and Washers
3/29/2017	McMaster-Carr	99.61	Epoxy and Nozzles
4/6/2017	McMaster-Carr	548.05	Pressure Chamber
4/10/2017	McMaster-Carr	467.28	Epoxy
Sub Total		1857.2	
Electronics			
2/24/2017	DKC Digi Key Corp	160.26	Power Amps, Resistors, etc
Sub Total		160.26	
Total Cost		5121.82	

B. Hydrophone Specification Sheets

RESON

Hydrophone TC4034

Ultra Broad-band Spherical

TC4034

- Omnidirectional in the full frequency range
- Long term stability
- Extreme Wide frequency range
- Durable construction
- Individually calibrated

The TC4034 broad band spherical hydrophone provides uniform omni-directional characteristics over a wide frequency range of 1Hz to 480kHz.

The overall receiving characteristics makes the TC4034 an ideal transducer for making absolute underwater sound measurements up to 480kHz. The wide frequency range also makes the TC4034 perfect for calibration purposes, particularly in higher frequencies.

TECHNICAL SPECIFICATIONS	
Usable Frequency range:	1Hz to 470kHz (+3, -10dB)
Linear Frequency range:	1Hz to 250kHz (+2, -4dB)
Receiving Sensitivity: (re 1V/µPa)	-218dB ±3dB (at 250Hz)
Horizontal directivity:	Omnidirectional ±2dB (at 100 kHz)
Transmitting sensitivity:	122dB ±3dB (typical) re 1µPa/V at 1m at 100kHz
Vertical directivity:	>270° ±3dB (at 300kHz)
Nominal Capacitance:	3nF
Operating Depth:	900m
Survival Depth:	1000m
Operating Temperature range:	-2°C to +80°C
Storage Temperature range:	-40°C to +80°C
Weight incl. cable,(in air):	1.6 kg
Cable (length and type):	Standard 10m shielded pair DSS-2MIL-C915. Optional cable length available on request
Encapsulating Material:	Special formulated NBR
Metal body:	Alu-bronze - AlCu10Ni5Fe4
Connector type:	BNC

NBR means Nitrile Rubber

The NBR rubber is first of all resistant to sea and fresh water but also resistant to oil. It is limited resistant to petrol, limited resistant to most acids and will be destroyed by base, strong acids, halogenated hydrocarbons (carbon tetrachloride, trichloroethylene), nitro hydrocarbons (nitrobenzene, aniline), phosphate ester hydraulic fluids, Ketones (MEK, acetone), Ozone and automotive brake fluid.

RESON Hydrophone TC4034

Ultra Broad-band Spherical

Documentation:

Vertical directivity:
At 250 kHz 100,200,300 kHz

Receiving sensitivity:
5 kHz to 500 kHz

Transmitting sensitivity:
5 kHz to 500 kHz

Horizontal directivity:
At 100, 200, 300 kHz

Impedance:
5 kHz to 500 kHz

Horizontal directivity pattern

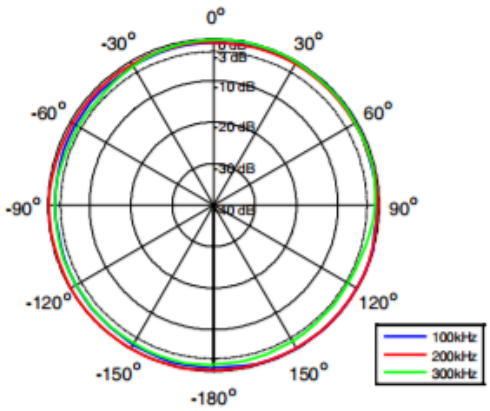

Receiving Sensitivity [dB re 1V/µPa @ 1m]

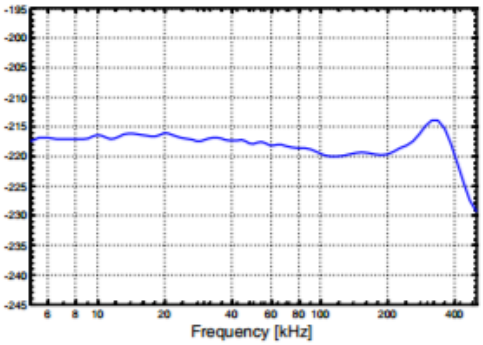

Transmitting Sensitivity [dB re 1µPa/V @ 1m]

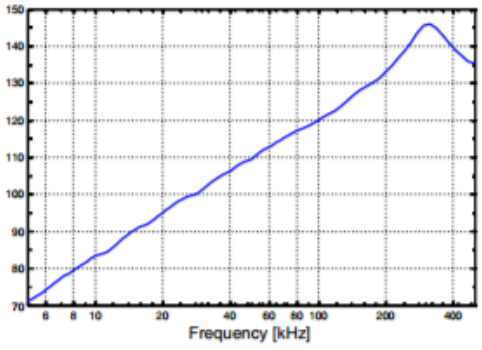

Impedance

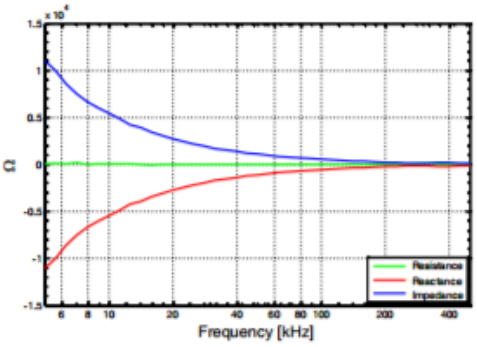

C. Polyurethane Elastomer Specification Sheet

BJB ENTERPRISES

ALIPHATIC & WATER CLEAR URETHANES

"Dedicated to QUALITY, SERVICE, SAFETY, and INNOVATION"

WC-565 A/B
WATER CLEAR SHORE 65 A
POLYURETHANE ELASTOMER

RoHS

WC-565 A/B is a two-part, clear, colorless aliphatic-based polyurethane elastomer. It is recommended for use whenever a flexible, permanently transparent elastomer is required. It is UV light and oxidation resistant and can be easily tinted or pigmented to clean bright colors.

WC-565 A/B does not contain MOCA, TDI, or MDA. In addition to being an excellent castable product, it also functions well as an adhesive for bonding various substrates.

PHYSICAL PROPERTIES	TEST METHOD	RESULTS
Hardness, Shore A	ASTM D2240-04e1	65 ± 5
Density (g/cc)	ASTM D792-00	1.02
Cubic Inches per Pound	N/A	26.54
Color/Appearance	Visual	Colorless/Clear
Tensile Strength (psi)	ASTM D412-98a(2002)e1	753
Elongation (%)	ASTM D412-98a(2002)e1	200
Tear Strength (pli)	ASTM D624-00e1	59
Shrinkage (in/in) linear	ASTM D2566 @ 1" depth	0.004
Dielectric Constant, 1 MHz	ASTM D150-87	3.483
Dissipation Factor, 1 MHz	ASTM D150-87	0.061

HANDLING PROPERTIES	Part A	Part B
Mix Ratio by weight	100	100
Mix Ratio by volume	95	100
Specific Gravity @ 77°F (25°C)	1.07	1.02
Color	Colorless	Colorless
Viscosity (cps) @ 77°F (25°C) Brookfield	4,725	310
Mixed Viscosity (cps) @ 77°F (25°C) Brookfield	1,100	
Work Time, 100g mass @ 77°F (25°C)	15 minutes	
Gel Time	20 minutes	
Demold Time @ 77°F (25°C)	6 – 8 hours	

Properties above are typical and not for specifications.

CURE SCHEDULE/HEAT CURING:

Most of the physical properties can be achieved in 5-7 days at 77°F (25°C). You may use your own post-cure schedule but the physical properties may vary from BJB's cure schedule of 1-3 hours at 77°F (25°C) followed by 16 hours at 160°F (71°C). Do not exceed curing temperatures of 200°F (93°C).

If you are using heat to accelerate the demold time, allow the part to cool down to ambient temperature before demolding.

NOTE:

The cure will be inhibited if cast against a tin catalyzed silicone RTV.

STORAGE AND HANDLING:

Store at ambient temperatures, 65-80°F (18-27°C). Unopened containers will have a shelf life of 6 months from date of shipment when properly stored at recommended temperatures. Purge opened containers with dry nitrogen before re-sealing.

PACKAGING	Part A	Part B	Cubic Inches per Kit
Gallon Kits	8 lbs.	8 lbs.	425
5-Gallon Kits	40 lbs.	40 lbs.	2,123
55-Gallon Drum Kits	400 lbs.	400 lbs.	21,232

SAFETY PRECAUTIONS:

Avoid contact with skin using protective gloves and protective clothing. Repeated or prolonged contact on the skin may cause an allergic reaction. Eye protection is extremely important. Always use approved safety glasses or goggles when handling this product. Use in well-ventilated areas. Avoid breathing vapors. If exposures cannot be kept at a minimum, a respirator may be necessary in addition to ventilation. The use of a positive pressure air supplied respirator is mandatory when airborne isocyanate concentrations are "not known" or exceeds OSHA TWA of 0.005 ppm. Air purifying, organic cartridge type respirators are not generally recommended to use when handling this material without implementation of an end of life service program. Observe OSHA regulations for respirator use (29 CFR 1910.134). Employers are responsible for selecting the correct respirator for each situation.

IF CONTACT OCCURS:

Skin: Immediately wash with soap and water. Remove contaminated clothing and launder before reuse. It is *not* recommended to remove resin from skin with solvents. Solvents only increase contact and dry skin. Seek qualified medical attention if allergic reactions occur.
Eyes: Immediately flush with water for at least 15 minutes. Call a physician.
Ingestion: If swallowed, call a physician immediately. Remove stomach contents by gastric suction or induce vomiting only as directed by medical personnel. Never give anything by mouth to an unconscious person.

Refer to the Material Safety Data Sheet before using this product.

Handling Guide

WC-565 Part A SDS

WC-565 Part B SDS

D. Silicone Specification Sheets

BJB ENTERPRISES

SILICONE CASTING RUBBERS

"Dedicated to QUALITY, SERVICE, SAFETY, and INNOVATION"

TC-5015 A/B
TRANSLUCENT SILICONE RUBBER

TC-5015 A/B is a room temperature, addition/platinum curing silicone rubber designed for making molds and parts. When used to make molds, the TC-5015 A/B is translucent enough to see through when casting into the mold cavity. This aids in developing void free surfaces on the casting. TC-5015 A/B is also commonly used to make ink stamp pads as well as other types of pressure pads.

PHYSICAL PROPERTIES	TEST METHOD	RESULTS
Hardness, Shore A	ASTM D 2240-04e1	15 ± 5
Density (g/cc)	ASTM D 792-00	1.06
Cubic Inches per Pound	N/A	26.2
Color/Appearance	Visual	Colorless/Translucent
Tensile Strength (psi)	ASTM D 412-98a(2002)e1	320
Elongation (%)	ASTM D 412-98a (2002)e1	350
Tear Strength (pli)	ASTM D 624-00e1 Die B	60
Shrinkage (in/in) linear	ASTM D2566 @ 1" depth	Nil

HANDLING PROPERTIES	Part A	Part B
Mix Ratio by weight	100	10
Specific Gravity @ 77°F (25°C)	1.07	0.97
Color	Colorless	Colorless
Viscosity (cps) @ 77°F (25°C) Brookfield	31,000	80
Mixed Viscosity (cps) @ 77°F (25°C) Brookfield	15,000	
Work Time, 100g mass @ 77°F (25°C)	25 minutes	
Gel Time	30 minutes	
Demold Time @ 77°F (25°C)	24 hours	

Properties above are typical and not for specifications.

INHIBITION:

Certain materials will cause inhibition or neutralization of the curing agent. These materials include condensation/tin cured based silicone, lacquer and enamel coatings, polyester-based products, copper or copper containing metals, some SLA resins, and natural rubbers like latex. Inhibition may easily be determined by brushing a small quantity of TC-5030 A/B over a localized area of the surface to be reproduced. If the TC-5015A/B is tacky or uncured after the cure time, then you know the mold surface is acting as an inhibitor. Molds made from wood, plaster, steel, aluminum, or plastic should not cause inhibition if they are clean. To insure against possible problems, it is advisable to spray a barrier film over any questionable surfaces. This is the best way of treating clays and other surfaces that cause inhibition. Contact BJB for recommended products.

STORAGE:

Store ambient temperatures, 65-80°F (18-27°C). Unopened containers will have a shelf life of 12 months from date of shipment when properly stored at recommended temperatures. Purge opened containers with dry nitrogen before re-sealing.

PACKAGING	Part A	Part B	Cubic Inches Per Kit
Quart Kits	2 lbs.	3.2 oz.	58
Gallon Kits	8 lbs.	13 oz.	231
5-Gallon Kits	40 lbs.	4 lbs.	1,153
55-Gallon Drum Kits	450 lbs.	45 lbs.	12,969

SAFETY PRECAUTIONS:

Use in a well-ventilated area. Avoid contact with skin using protective gloves and protective clothing. Repeated or prolonged contact on the skin may cause an allergic reaction.

Eye protection is extremely important. Always use approved safety glasses or goggles when handling this product.

IF CONTACT OCCURS:

Skin: Immediately wash with soap and water. Remove contaminated clothing and launder before reuse. It is *not* recommended to remove resin from skin with solvents. Solvents only increase contact and dry skin. Seek qualified medical attention if allergic reactions occur.

Eyes: Immediately flush with water for at least 15 minutes. Call a physician.

Ingestion: If swallowed, call a physician immediately. Remove stomach contents by gastric suction or induce vomiting only as directed by medical personnel. Never give anything by mouth to an unconscious person.

Refer to the Material Safety Data Sheet before using this product.

Silicone Handling Guide

TC-5015 Part A SDS

TC-5015 Part B SDS

E. Silicone Mold Process

1. Cut 4 walls and 1 base out of plexiglass.
    a. 2 walls are 5 in x 2 in and 2 walls are 2.5 in x 2 in
    b. 1 base is 5 in x 2 in
2. Hot glue walls and base together.
    a. Note: Make sure the connection of walls and base are strong and no cracks/holes are present, silicone will leak through any cracks/holes.

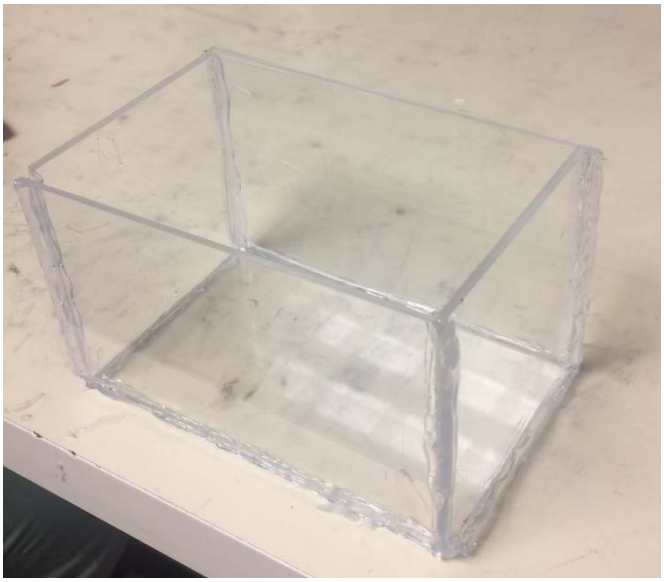

3. The silicone mold will be made in two parts. Cover base of box with oil based clay to eliminate volume of box that does not need to be filled with silicone. This clay will be taken out later and form the second half of the silicone mold.
4. Place a cylinder (3 in length, 1.5 in diameter) in box. This cylinder is the same size as the transducers.

5. Push smaller diameter of bolts into the clay around perimeter of box and put clay in hole on top of bolt.

6. Pour the two-part silicone into a cup as instructed in the material data sheets. Place the silicone in vacuum chamber. Repeatedly pull a vacuum on the silicone to eliminate bubbles.

7. Pour silicone into box.

8. Let silicone cure for 24 hours, as specified on the material data sheets.
9. Take box apart and remove the clay.
10. Reassemble plexiglass box around the first half of the silicone mold.
11. Spray top of half of silicone mold with mold release.
12. Ensure 1.5 in diameter cylinder is placed in half of mold.
13. Glue two plastic rods to middle of cylinder. This will create holes in the mold to pour the urethane in and let air out.
14. Pour silicone into box to create second half.
15. Let silicone cure for 24 hours.
16. Remove plastic rods from cylinder and take apart plexiglass box.

17. The two part silicone mold is complete.

F. Urethane Casting Process

1. Place assembled transducer in finished silicone mold.

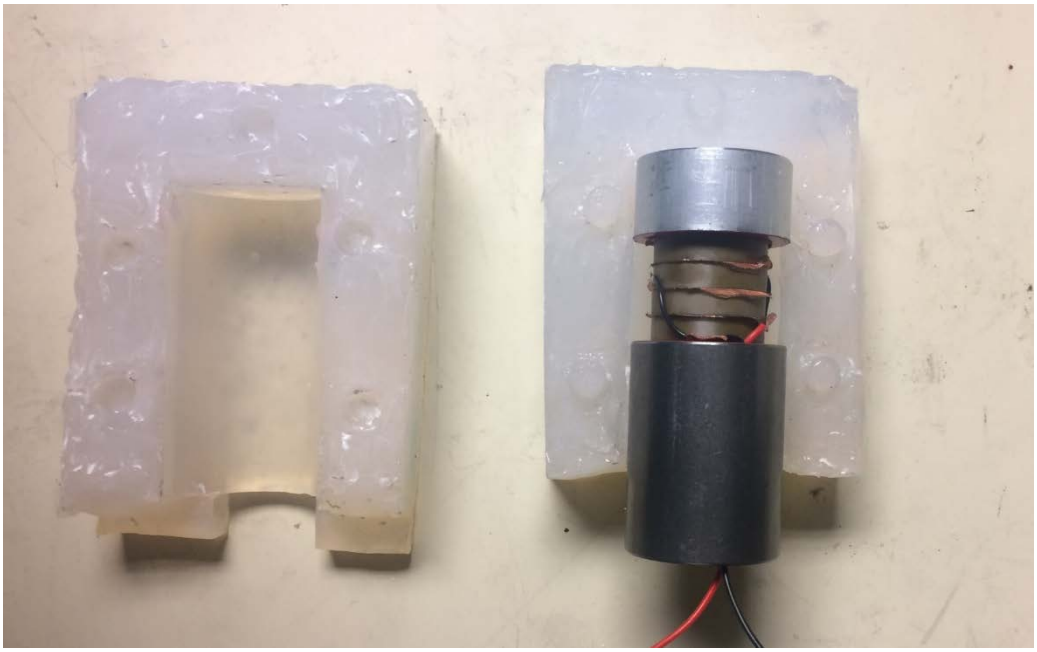

2. Place two halves of mold together and tightly wrap tape around silicone mold to ensure the mold will not expand or leak.
3. Mix the two-part urethane as specified on the material data sheets.
4. Place mixture into vacuum chamber and repeatedly draw a vacuum to remove bubbles.

5. Place straw in one of the holes in the silicone mold, used for the air output.

6. Pour urethane mixture into frosting bag that has a hole and straw attached to it, as shown below.

7. Pour urethane mixture into the hole in silicone mold without a straw until excess urethane is flowing up air output straw (mold is filled with urethane and no more air is present to exit).

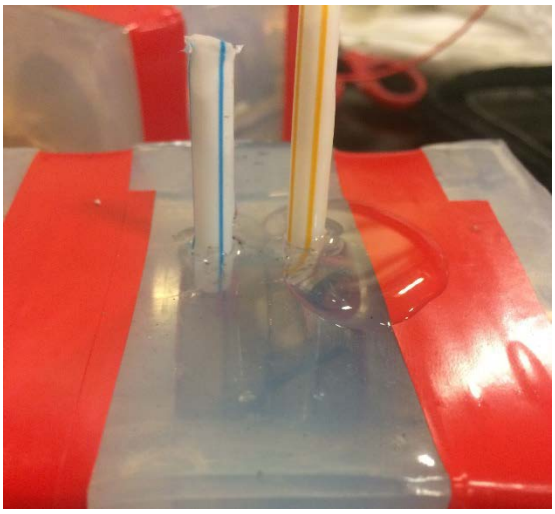

8. Place mold in pressure chamber at 55 psi for 6-8 hours, as specified on the material data sheet.
9. Remove mold from pressure chamber.
10. Unwrap tape and take transducer out of mold.
11. If the ceramic ring and wiring is not completely covered, fill the holes with urethane and place back in pressure chamber for curing.

G. Transducer Design MATLAB Code

initialize physical constants

```
f=15000; % frequency in Hz
rho_a=2700; % density of 6061 aluminum in kg/m^3
rho_s=8000; % density of 304 Stainless Steel in kg/m^3

rh=(0.25/2)*(2.54)/100; % radius of 1/4-20 tapped hole in head mass
dh=0.02; % depth of 1/4-20 screw tap

Ca=6320; % Speed of sound in aluminum in m/sec
Cw=1500; % Speed of sound in water in m/sec
```

calculate stiffness of cermaic

```
E=7.8e10; % Young's Modules in N/m^2 http://bostonpiezooptics.com/ceramic-materials-pzt
http://bostonpiezooptics.com/assets/pdf/Equiv_Ceramic_Matls.pdf
R_ceramic_outer=28/1000/2; % Outer radius of ceramic ring in meters
R_ceramic_inner=9/1000/2; % Inner radius of ceramic ring in meters
L=6/1000; % height of ceramic ring in meters

A=(R_ceramic_outer^2-R_ceramic_inner^2)*pi;

ko=A*E/L; % spring constant of one ceramic ring

number_rings=5; % number of ceramic rings used in series
k=ko/number_rings; % equivilent spring constant of ceramic rings in series

%Iteration 2

Wn_data=[7340 7340 7250];
Wn=mean(Wn_data); % angular freqency
HM_mass=0.16111 % kg

k=((Wn*2*pi)^2)*HM_mass
```

First Iteration

```
Ho=Ca/(8*f); %intial guess for headmass height in meters
ro=sqrt((k/(4*(f^2)*rho_a*(pi^3)*Ho))+((rh^2)*dh/Ho)); %intial radius
do=2*ro;
if ro>=Cw/(4*f)
    fprintf('The Diameter of the Tranducer Exceeds Half the \nWavelength of the Speed of
Sound in Water \nEither Increase the Number of Ceramic Rings or Directly Reduce r')
else
    fprintf('The Calculated Value for the Radius is Valid')
end
```

Second Iteration (diameter was found to be 29.6mm and was rounded up to 30mm and 40mm)

```
r1=30/2/1000; % radius of headmass in meters
% r2=40/2/1000; % radius of headmass in meters
r2=(1+5/8)*2.54/100/2; % radius of headmass in meters

H1=((k/(4*(f^2)*rho_a*(pi^3)))+((rh^2)*dh))*(1/r1^2);
H2=((k/(4*(f^2)*rho_a*(pi^3)))+((rh^2)*dh))*(1/r2^2);
```

Find Height of tail mass (mass of tail mass >= 4*mass of head mass)

```
rh_TM=.676/2/100; % radius of hole for bolt
rc=.1905/2/100; % radius of the counterbore on bottom of tailmass in meters
dc=.15/2/100; % depth of counterbore on bottom of tailmass in meters

H1_TM=((rh_TM^2)*rho_s*dc+(r1^2)*4*H1*rho_a+(rc^2)*rho_s*dc)/(rho_s*(r1^2-rh_TM^2)); %
Height of tailmass in meters
H2_TM=((rh_TM^2)*rho_s*dc+(r2^2)*4*H2*rho_a+(rc^2)*rho_s*dc)/(rho_s*(r2^2-rh_TM^2)); %
Height of tailmass in meters
```

Published with MATLAB® R2016a

H. Impedance Curve MATLAB Code

Pinger Data Acquisition

```
clear all; close all;

% The following command should return info about installed NI DAQ cards
% d=daq.getDevices
%
% important note: the first line of the result from the command above
% should be something like:
%    ni: National Instruments USB-6361 (BNC) (Device ID: 'Dev1')
% 'Dev1' is the name of the device according to matlab, and you'll see this
% used below.

% create the daq session
s = daq.createSession('ni');
```

Define Test Parameters

```
VPP = 10; % Volts Peak to Peak of function generator
SampleDuration = 2; % Set durration of sampling
Startf = 10*10^2; %[Hz]
Stopf = 20*10^3; %[Hz]

% add channel 0
fs = 500000;
s.Rate = fs;    % sampling frequency
s.DurationInSeconds = SampleDuration;   % sampling duration
ch0.Range = [-VPP/2 VPP/2]; % change the input range to +/- 2.5 volt
ch0 = s.addAnalogInputChannel('Dev1',0,'Voltage');
ch1.Range = [-VPP/2 VPP/2]; % change the input range to +/- 2.5 volt
ch1 = s.addAnalogInputChannel('Dev1',1,'Voltage');

% acquire data
sample = 1;
% freq = 100:100:20000;

for i = 1:sample

    field = (['Sample',num2str(i),'']);

     %ff = freq(i);

    %disp(['change frequency to ' num2str(ff) ' Hz, then hit a key'])
%     pause
         close all

    % acquire data:
    T = now;      % this is the time of acquisition; this will be recorded in the
filename
    [data,time] = s.startForeground;  % this starts the acquisition
```

```
    % plot the data
    subplot(211)
    plot(time,data(:,1))  % time series
    xlabel('time (s)')
    ylabel('amplitude (volts)')
    title('channel 0')

    subplot(212)
    plot(time,data(:,2))  % time series
    xlabel('time (s)')
    ylabel('amplitude (volts)')
    title('channel 1')

    dataset.(field).data = data;
    dataset.(field).time = time;
    dataset.(field).T = T;
    dataset.(field).fs = fs;
    dataset.(field).SampleDuration = SampleDuration;
    dataset.(field).Startf = Startf;
    dataset.(field).Stopf = Stopf;

end

% save data
disp('Saving data...')
%eval(['save Sample_' num2str(i) '_' datestr(T,'yyyymmdd') 'dataset'])
filename = (['Test_1_OilFill' datestr(T,'yyyymmdd') '.mat']);
save(filename, 'dataset');
```

Check Plots

```
load('Prototype3_4rings_sixwashers_final_design420161208.mat')
Startf = 10*10^2; %[Hz]
Stopf = 20*10^3; %[Hz]
Samples = 1;

field = (['Sample1']);
                % Data For visualization
                data = dataset.(field).data;
                % data = data(1:100000,:);
                time = dataset.(field).time;
                T = dataset.(field).T;
                fs = dataset.(field).fs;
E1 = fftshift(fft(data(:,1)));
E2 = fftshift(fft(data(:,2)));
tau = 1/fs/2;
f = linspace(-fs/2,fs/2,length(E1));
phi = 2*pi*f*tau;
E2 = E2./exp(j*phi');
I = E2/3300;
Ec = E1-E2;
Z = Ec./I;
Y = 1./Z;
```

```
figure(1)
plot(f,imag(Y(:,1))/2/pi./f','-.');
title('Suseptance vs Frequency')
xlim([Startf Stopf])
grid on; grid minor;

figure(2)
plot(f,real(Y(:,1)),'-');
xlim([Startf Stopf])
title('Conductance vs. Frequency','fontsize',16)
ylabel('Amplitude [S]','fontsize',14)
xlabel('Frequency [Hz]','fontsize',14)
grid on; grid minor;

Ymean = mean(Y(:,1:Samples),2);
        Zmean = mean(Z(:,1:Samples),2);

        % Aquire frequency range from 100 to 10000 Hz.
        fminindx = find(ceil(f) == Startf);
        fmaxindx = find(ceil(f) == Stopf);
        fnew = f(fminindx:fmaxindx);

        % redefine data for this range
        Zmeannew = Zmean(fminindx:fmaxindx);
        Ymeannew = Ymean(fminindx:fmaxindx);

figure(3)
plot(fnew,real(Zmeannew),'-',fnew,imag(Zmeannew),'r-.');
    grid on; grid minor;
    xlabel('Frequency [Hz]');
    ylabel('Amplitude [/Omega]');
    title(['Resistance and Reactance vs. Frequency ']);
    legend('Resistance','Reactance')
```

Published with MATLAB® R2016a

I. Signal Processing MATLAB Code

First author on this code is Thomas Weber (Weber, 2017)

```
clear all; close all;

filelocation = '..';
addpath 'EK80Matlab\'
```

Read in the raw data

```
npingsmax = 1e6;
[fnames,fpath,FilterIndex] = uigetfile(strcat(filelocation,'\*.raw'),'Select raw
files','MultiSelect','on');
if iscell(fnames)
    nfiles = length(fnames);
else
    nfiles = 1;
end


for nf = 1:nfiles,
    if (nfiles>1)
        filename = [fpath fnames{nf}];
    else
        filename = [fpath fnames];
    end

    %%%%%%%%%%%%%%%%%%%
    % Read "npingsmax" pings from file "filename"
    disp(filename)
    tic

    [configdata,filterdatavec,sampledatamat,NMEA] = readrawEK80(filename,npingsmax);
    NumPings = length(sampledatamat);


    for i = 1:NumPings
        s = sampledatamat(i).complexsamples;

        % extract individual channels
        s1(:,i) = s(:,1);
        s2(:,i) = s(:,2);
        s3(:,i) = s(:,3);
        s4(:,i) = s(:,4);
        sAll(:,i) = sum(s,2);

        % match filter
        transceiver = gettransceiver(configdata,filterdatavec,sampledatamat,1,1,i,1);
        [tx,ytx] = createtx(transceiver);
        ytxauto = conv(ytx,flipud(conj(ytx)))/norm(ytx)^2;
        s1_mf(:,i) = conv(s1(:,i),flipud(conj(ytx)))/norm(ytx)^2;
```

```
        s2_mf(:,i) = conv(s2(:,i),flipud(conj(ytx)))/norm(ytx)^2;
        s3_mf(:,i) = conv(s3(:,i),flipud(conj(ytx)))/norm(ytx)^2;
        s4_mf(:,i) = conv(s4(:,i),flipud(conj(ytx)))/norm(ytx)^2;
        sAll_mf(:,i) = s1_mf(:,i) + s2_mf(:,i) + s3_mf(:,i) + s4_mf(:,i);
        % remove match filter delay
        delay_match = length(ytx);
        s1_mf(1:end-delay_match,i) = s1_mf(delay_match:end-1,i);
        s2_mf(1:end-delay_match,i) = s2_mf(delay_match:end-1,i);
        s3_mf(1:end-delay_match,i) = s3_mf(delay_match:end-1,i);
        s4_mf(1:end-delay_match,i) = s4_mf(delay_match:end-1,i);

        % shift to baseband
        sampint = sampledatamat(1).sampleinterval;
        fs = 1/sampint;
        t = (1:length(s1_mf(:,1)))'/fs;
        s1_mf(:,i) = s1_mf(:,i).*exp(-j*2*pi*15000*t);
        s2_mf(:,i) = s2_mf(:,i).*exp(-j*2*pi*15000*t);
        s3_mf(:,i) = s3_mf(:,i).*exp(-j*2*pi*15000*t);
        s4_mf(:,i) = s4_mf(:,i).*exp(-j*2*pi*15000*t);


    end
```

```
C:\Users\Langdon\Documents\Senior Year\Senior Design
Project\HarborTesting\HarborTest_ch2and4_1kw_8ms_11kto18k-D20170414-T154950.raw
Finished reading file
```

```
    figure(1)

    pings = 1:903;
    r = (1:length(s2_mf))/fs*750;
    imagesc(pings,r,20*log10(abs(s2_mf+s4_mf)));
    caxis([-85 -50])
    a = axis;
    axis([a(1) a(2) 10 60])
    colormap copper
    title('Unfiltered Raw Data')
    xlabel('Ping Number')
    ylabel('Range [m]')

    % filter the data to get rid of the noise
    %[B,A] = butter(7,[3000 7000]/fs,'stop');
    [B,A] = butter(7,2500/fs);
    s1_mf_filt = filtfilt(B,A,double(s1_mf));
    s2_mf_filt = filtfilt(B,A,double(s2_mf));
    s3_mf_filt = filtfilt(B,A,double(s3_mf));
    s4_mf_filt = filtfilt(B,A,double(s4_mf));

    [B,A] = butter(7,.1,'high');
    figure(2)
    imagesc(pings,r,20*log10(abs(s2_mf_filt + s4_mf_filt)))
    caxis([-45 -12.5])
    axis([a(1) a(2) 10 60])
```

```
    colormap copper
    title('Filtered Data')
    xlabel('Ping Number')
    ylabel('Range [m]')

    % take out the range dependency (sort of)
    norm = 30*log10(r')*ones(1,903);
    figure(3)
    imagesc(pings,r,norm + 20*log10(abs(filtfilt(B,A,abs(double(s2_mf))))))
%abs(double(s2_mf)+double(s4_mf))))))
    xlabel('Ping Number')
    ylabel('Distance [m]')
    title('Side-Scan SONAR Backscatter')
    caxis([-45 -12.5]);axis([a(1) a(2) 10 60]); colormap copper
```

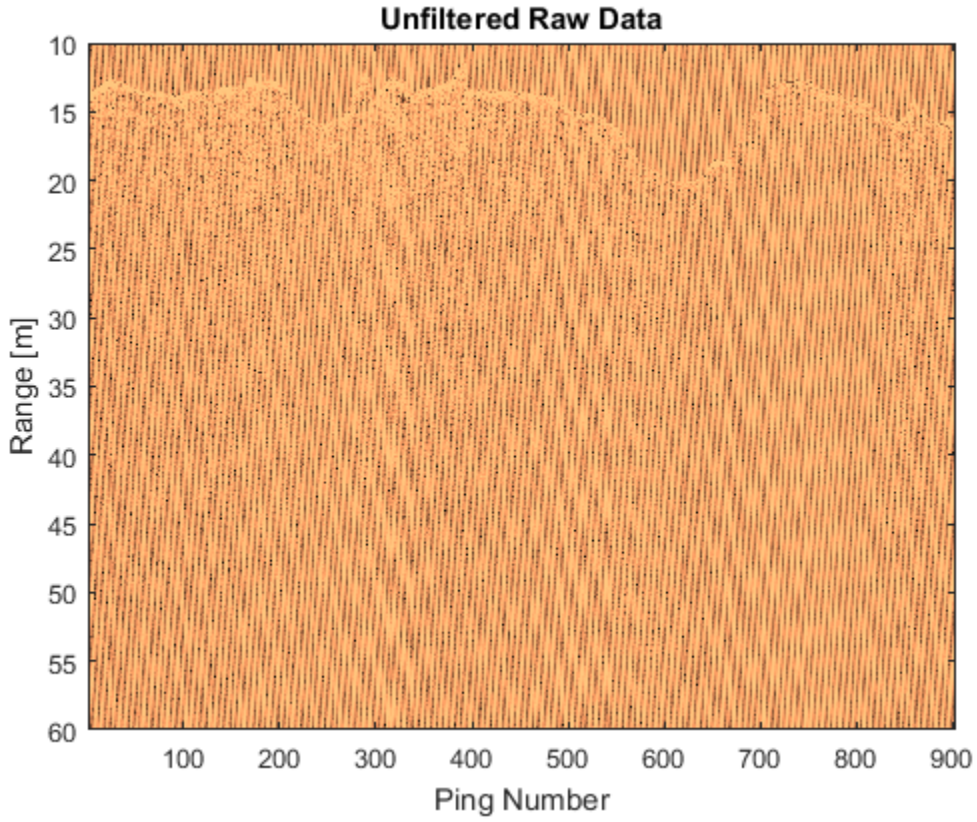

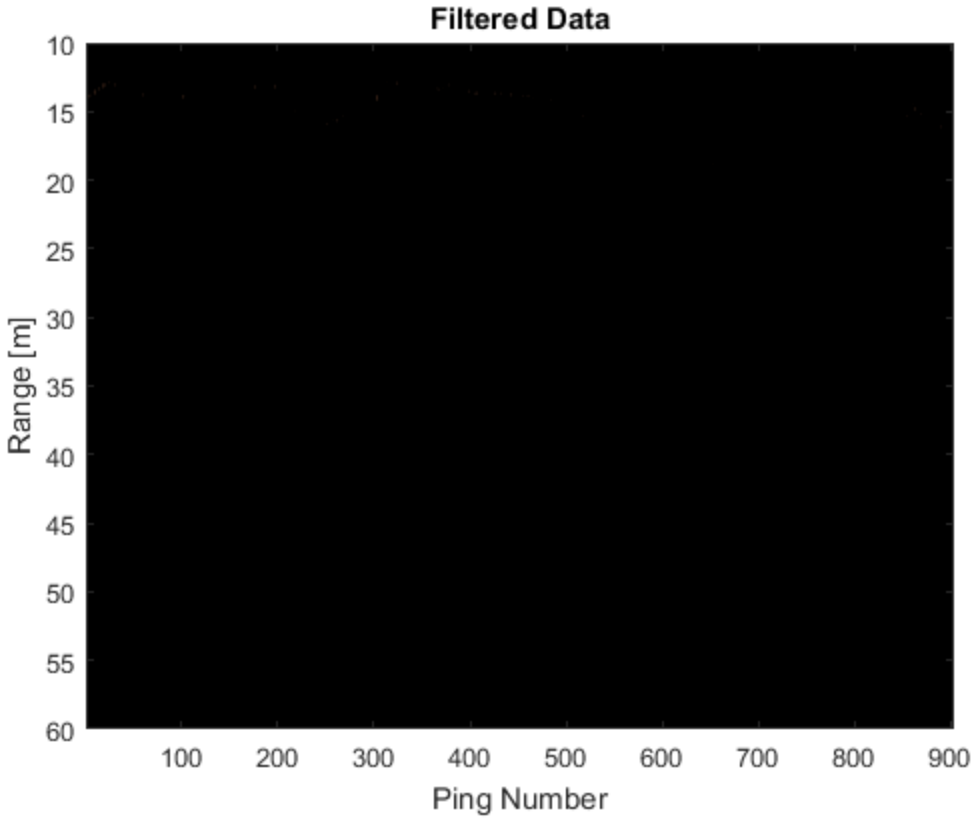
Filtered Data
Range [m]
10
15
20
25
30
35
40
45
50
55
60
100
200
300
400
500
600
700
800
900
Ping Number

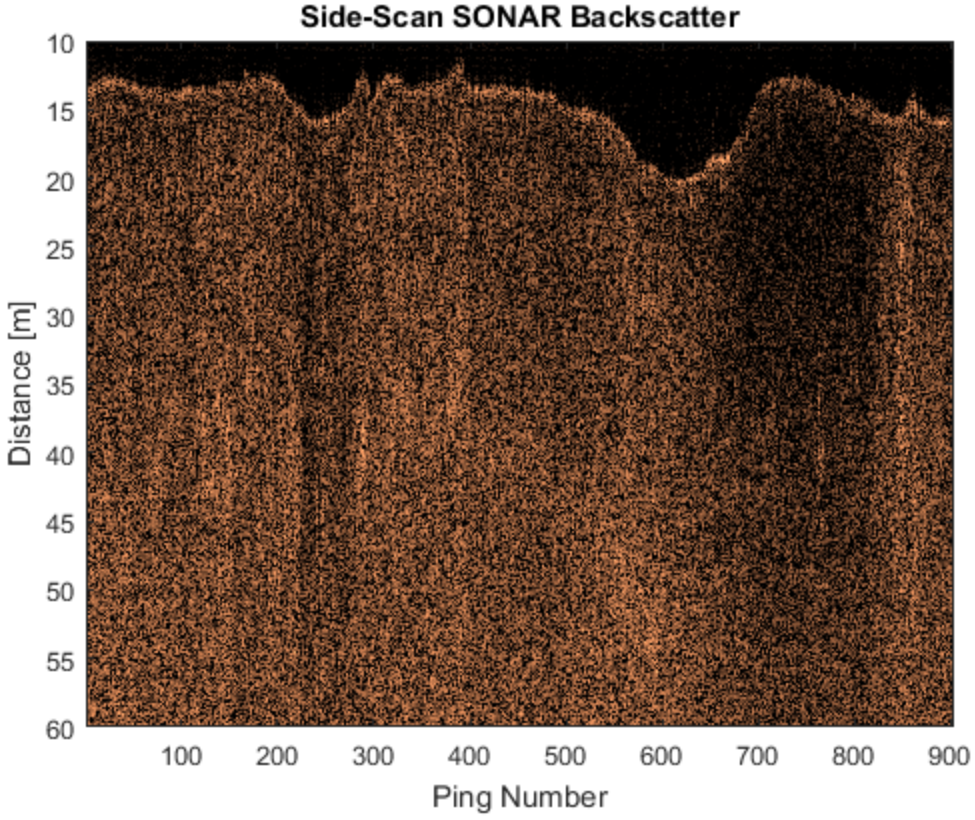
Side-Scan SONAR Backscatter
Distance [m]
10
15
20
25
30
35
40
45
50
55
60
100
200
300
400
500
600
700
800
900
Ping Number

```
    figure(4)
    imagesc(pings,r,norm + 20*log10(abs(filtfilt(B,A,abs(double(s2_mf))))))
%abs(double(s2_mf)+double(s4_mf))))))
    xlabel('Ping Number')
    ylabel('Distance [m]')
    title('Backscatter Sand Waves')
    caxis([-31 -24]);axis([40 270 10 30]); colormap copper
    %phi = angle(double(s2_mf_filt).*conj(double(s4_mf_filt)));
```

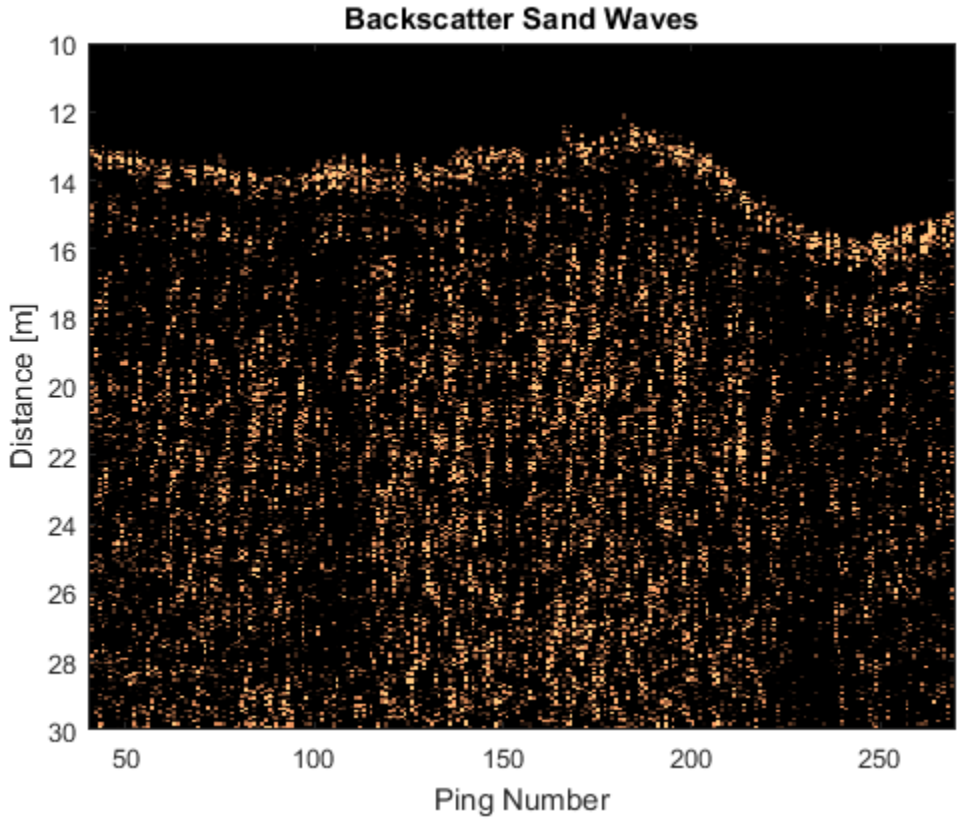


```
end
```

Spectogram Plot

```
%unfiltered data
figure(5)
spectrogram(double(s2_mf(:,floor(1)))+double(s4_mf(:,floor(1))),25,10,100,'yaxis',150000/
(2*pi))
caxis([-140 -90])

%filtered data
figure(6)
spectrogram(double(s2_mf_filt(:,floor(1)))+double(s4_mf_filt(:,floor(1))),25,10,100,'yaxi
s',150000/(2*pi))
caxis([-140 -90])
```

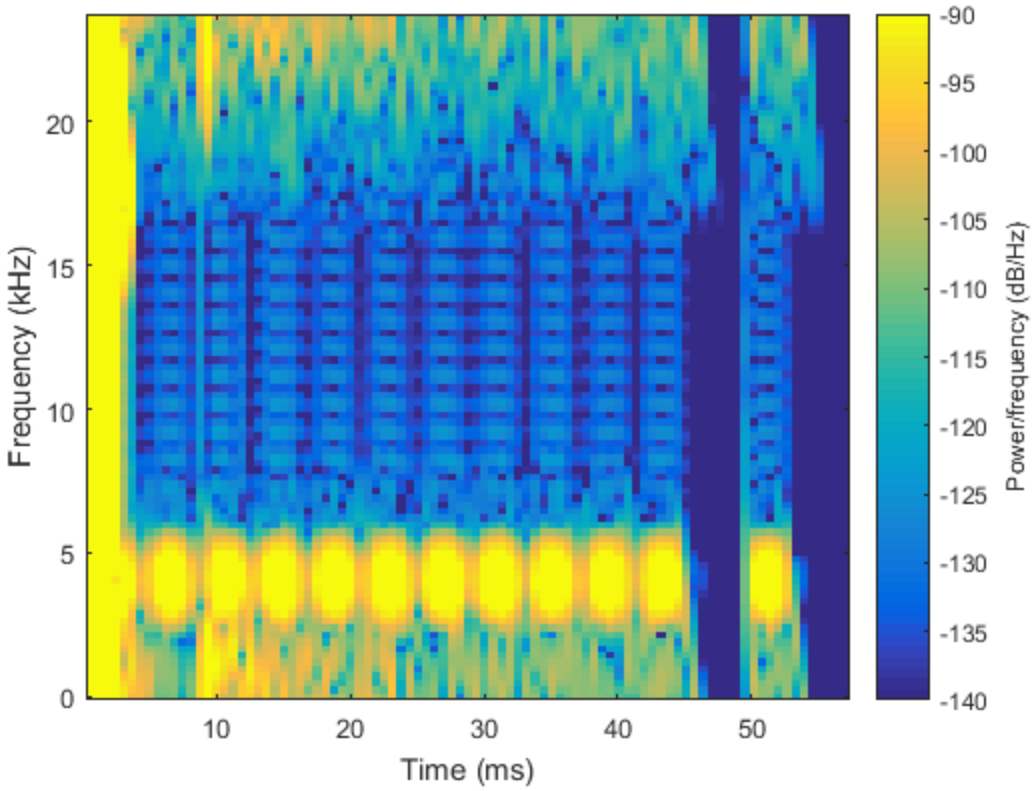

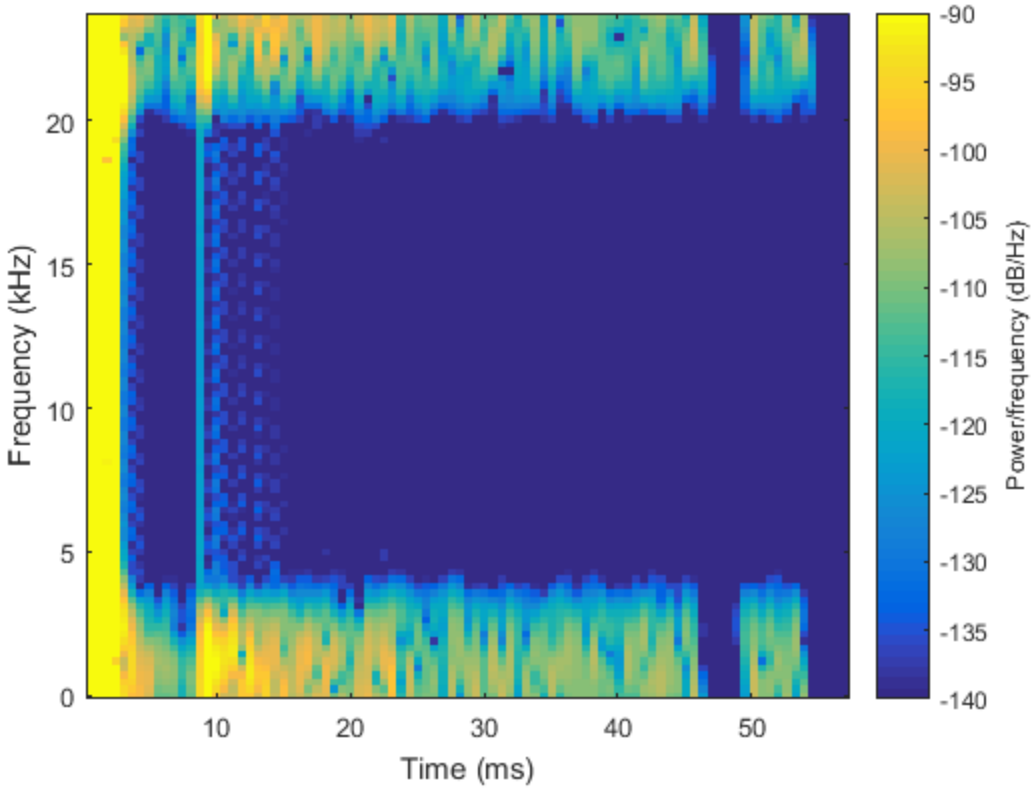

Published with MATLAB® R2016a